Summer 2018

Surface-Enhanced Raman Spectroscopy Studies of Organic Dyes for Art Conservation and Ph Sensing Applications

Shelle Nicholle Butler

College of William and Mary - Arts & Sciences, snbutler01@email.wm.edu

Surface-Enhanced Raman Spectroscopy Studies of Organic Dyes for Art Conservation and pH Sensing Applications

Shelle N. Butler

Richmond, Virginia

B.S. Chemistry, Virginia Commonwealth University, 2016
B.S. Forensic Science, Virginia Commonwealth University, 2016

A Thesis presented to the Graduate Faculty of The College of William & Mary in Candidacy for the Degree of
Master of Science

Department of Chemistry

College of William & Mary
May 2018

APPROVAL PAGE

This Thesis Here is submitted in partial fulfillment of the requirements for the degree of

Master of Science

Shelle Nicholle Butler

Approved by the Committee, April 2018

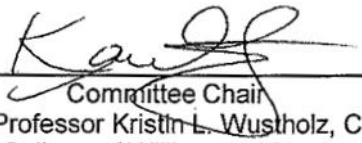

Committee Chair
Associate Professor Kristin L. Wustholz, Chemistry
College of William and Mary

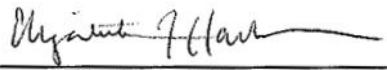

Professor Elizabeth J. Harbron, Chemistry
College of William and Mary

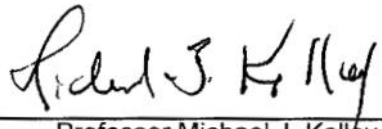

Professor Michael J. Kelley, Applied Science
College of William and Mary

ABSTRACT

Surface-enhanced Raman scattering (SERS) spectroscopy is a powerful analytical technique with widespread applications. In this work, the application of SERS in the fields of art conservation and pH sensing are reviewed. First, the theory of this unambiguous and ultrasensitive technique is explained. Next, a review of the pedagogical journey in art conservation research through the lenses of undergraduates is offered in Chapter 2. Finally, an investigation in pH sensing SERS is explored pursuing developing a SERS pH sensitive probe while offering new insight into SERS capabilities and the relationship between analyte and nanoparticle.

TABLE OF CONTENTS

ACKNOWLEDGEMENTS

I would like to express my sincere appreciation to Professor Kristin L. Wustholz, under whose guidance this investigation was conducted, for her patience, guidance and criticism throughout the investigation. The author is also indebted to Professors Elizabeth J. Harbron and Michael J. Kelley for their careful reading and criticism of the manuscript.

I would also like to take the opportunity to thank all of the amazing undergraduate researchers in our lab, whose curiosity allowed me to gain a better understanding of research and to form better mentor/mentee relationships.

I would also like to my graduate peers for helping me maintain my sanity throughout the challenges encountered along the way.

Chapter 1: SERS Theory and Background

Raman Scattering

Two ways in which light can scatter include: Rayleigh scattering and Raman scattering. In Rayleigh scattering, the incident photon energy ($h\nu_0$) is the same energy as the scattered photon energy. Scattered light has a higher propensity towards the conserved Raleigh scattering effect. However, a small amount of light energy, 1 in 10^{10} incident photons,[1] may be scattered at a different energy relative to inherent frequency in an effect known as Raman scattering. Whereas Rayleigh scattering is the elastic scattering of light, Raman scattering is the inelastic scattering of light. When light acts upon a molecule, an oscillating field is applied which momentarily causes a distortion in the electron cloud creating a higher energy state than its normal vibrational states, referred to as a "virtual state." Upon the return to ground state, the minute energy difference between the incident light energy and the scattered photon energy is known as the Raman shift ($h\nu'$). The energy shift is indicative of the characteristic molecular vibrational modes.

Raman spectroscopy relies on the polarizability of a molecule. Polarizability is the relative tendency of the charge distribution shape to change and shift when an electric field is applied. The applied electric field generates an induced dipole that radiates photons without exchanging energy (Rayleigh scattering) or with exchanging energy (Raman scattering) with the vibrational modes within the molecule. The induced polarization (P) is expressed as:

$$P = \alpha E \quad (1)$$

where α is the polarizability, or the ease of an atom's electron cloud to become distorted from its normal shape by an applied electric field, E. The electric field is governed by:

$$E = E_0 \cos 2\pi \nu_0 t \quad (2)$$

where ν_0 refers to the frequency of the excitation light source (e.g. a laser). The linear relationship between the laser intensity of the excitation source and the induced polarizability is revealed by combining Equations 1 and 2. Since Raman spectroscopy is a vibrational spectroscopic technique, as visualized in the simple Jablonski diagram in Figure 1, it is applied to reveal a characteristic structural fingerprint, which can be utilized to identify molecules. The normal modes (Q_j) that make up the characteristic molecular vibrations are expressed by:

$$Q_j = Q_j^o \cos 2\pi \nu_j t \quad (3)$$

where ν_j is the characteristic vibrational frequency and Q_j^o is the static molecule. Both corresponding to the *jth* normal modes for which there are 3*N*-6 normal modes in nonlinear molecules and 3*N*-5 normal modes in linear molecules with *N*, atoms. The polarizability of the molecular electrons is thereby modified by the molecular vibrations such that:

$$\alpha = \alpha_0 + \left(\frac{\delta \alpha}{\delta Q_j}\right) Q_j + \cdots \quad (4)$$

Combining the terms presented in Equations 1-4, yields the following:

$$P = \alpha_0 E_0 \cos 2\pi\nu_0 t + E_0 Q_j^o \left(\frac{\delta\alpha}{\delta Q_j}\right) \frac{\cos 2\pi(\nu_0+\nu_j)t + \cos 2\pi(\nu_0-\nu_j)t}{2} \quad (5)$$

which demonstrates that light is scattered at three separate frequencies. The first scattering frequency presented in the first term of Equation 5 denotes elastic scattering (Rayleigh) as shown in Figure 1. The combined second and third terms conceptualize Raman scattering considering both anti-Stokes Raman scattering $(\nu_0 + \nu_j)$ and Stokes Raman scattering $(\nu_0 - \nu_j)$. From Equation 5, it is evident that Rayleigh scattering is more intense relative to Raman scattering.

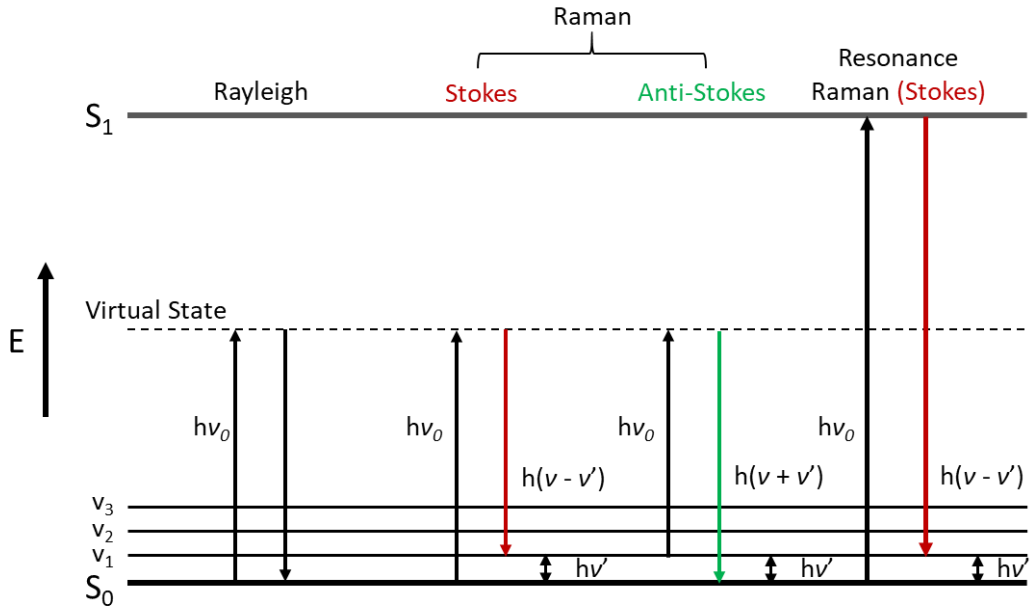

Figure 1. Jablonski energy diagram comparison of Rayleigh scattering and Raman scattering as depicted by the characteristic Raman vibrational shift (hν' or hν$_j$).

Typically, under standard conditions, molecules populate a ground vibronic state. When the incident photon interacts with the molecule, the photon may lose energy equal to the vibrational transition of the molecule resulting in a decreased scattered photon energy (i.e. a Stokes shift). If the molecule occupies an excited vibrational state, then the photon may gain energy when scattered leading to an anti-Stokes shift. When the incident frequency of the applied field matches the electronic resonance of the molecule then the conditions are met for resonance Raman scattering, which could lead to enhanced Raman signals.

The Raman scattering intensity (I_R), which is the number of photons scattered is given as:

$$I_R \propto (\nu_0 \pm \nu_j)^4 \alpha_j^2 Q_j^2 \quad (6)$$

The intensity of scattered photons is plotted against the energy of the scattered photons, expressed in wavenumbers, to produce a Raman spectrum.

Raman spectroscopy is an incredibly useful analytical technique for the identification of organic, inorganic, and biological samples, which can be complicated for other techniques due to interferences caused by complex matrices. The technique is applied to gases, liquids, and solids, including thin films and powders. Raman spectroscopy is a complimentary analytical technique to infrared (IR) spectroscopy. IR spectroscopy relies on the existence of a dipole moment, a separation of charge character within a molecule. The

principle selection rule for Raman requires a finite change in polarizability during the molecular vibration, $\left(\frac{\delta\alpha}{\delta Q_j}\right) \neq 0$. Even if the molecule is polarizable, certain analytes can encounter obstacles with Raman scattering. For example, Raman scattering faces major obstacles when applied to organic dyes: the weakness of scattering intensity, competitive effects with fluorescence, and not all modes may be Raman active. Even though other techniques have been incorporated to regain the lost intensity (e.g. FT-Raman), another method emerged in the 1970's to provide a remarkably enhanced Raman signal.

Surface-Enhanced Raman Scattering (SERS)

Over 40 years ago, Fleischmann and colleagues reported unusually intense Raman scattering from pyridine adsorbed to electrochemically roughened silver electrodes.[2] At the time, the authors believed that the increased surface area generated the enhancement due to the surface roughening process. Unknowingly, the discovery marked the first published observed SERS. Just a few years following Fleischmann's observation, Jeanmarie and Van Duyne and Albrecht and Creighton independently demonstrated that the signal enhancement is due to electromagnetic (EM) and chemical mechanisms.[3,4]

SERS works by two known mechanisms: chemical and EM enhancements. The chemical enhancement is attributed to charge transfer

between the chemisorbed species to the metal nanoparticle and is a minor component that has a weak enhancement on the order of $10^{2.5}$ The fluorescence of the molecule is quenched due to energy transfer to the metal.[6]

However, the majority of the overall signal enhancement is attributed to the EM contribution, which produces signal intensity increases from 10^4 to 10^{14},[5] the higher end is indicative of resonance Raman scattering. The mechanism is due to the optical properties of nanostructured metallic surfaces. The main optical property is referred to as localized surface plasmon resonance (LSPR) effect. LSPR is a phenomenon that occurs due to light interacting with particles much smaller than the incident wavelength. As the light interaction occurs, surface electrons oscillate as the electromagnetic field is applied to the metal nanoparticles leading to a plasmon. The plasmon oscillates locally about the surface of the nanoparticle with a resonance frequency, referred to as LSPR as shown in Figure 2.[5,7,8]

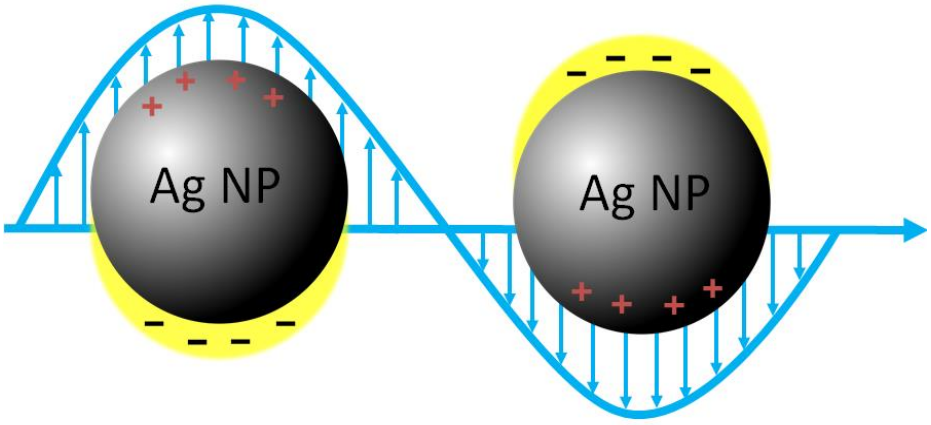

Figure 2. The signal enhancement due to oscillations of surface electrons (yellow) when an electric field (blue) is applied to metal nanoparticles generating LSPR.

The EM enhancement can be defined by an intrinsic enhancement factor (*EF*). The *EF* of a given signal can be expressed relative to the intensity of its normal Raman intensity as:

$$EF = \frac{|E_{out}|^2 |E'_{out}|^2}{|E_0|^4} = \frac{I_{SERS}/N_{SERS}}{I_{NR}/N_{NR}} \quad (7)$$

where the EM field intensity at the surface of the sphere ($|E_{out}|^2$) and the intensity of the Raman scattering ($|E'_{out}|^2$) are enhanced and scaled by the incident field intensity ($|E_0|^4$).[7] The *EF* is simply expressed by the SERS intensity (I_{SERS}) relative to the normal Raman intensity (I_{NR}).[7] To produce a significant EF, nanoparticles made from noble metals (e.g. silver, gold, or platinum) are added to the surface of the sample to serve as antennae that amplify the Raman signal and subdue interference caused by fluorescence. Even though other metals can be used to provide the surface, however, silver characteristically provides the largest enhancement factors.[9]

In 1982, Lee and Meisel published a method of synthesizing powerful citrate-reduced silver sols.[10] The Lee-Meisel method of silver nanoparticle (AgNP) synthesis is widely used for its simplicity of producing generally spherical nanoparticles. Lee-Meisel AgNPs offer higher SERS efficiency when partially aggregated, due to the formation of “hot spots” of large field enhancements.[11] When the chemisorbed analyte is localized in the LSPR region a “hot spot” is produced, Figure 3.[5,7,12] The hot spot is the area where

the SERS signal is optimally enhanced to reveal the characteristic chemical fingerprint of the analyte.

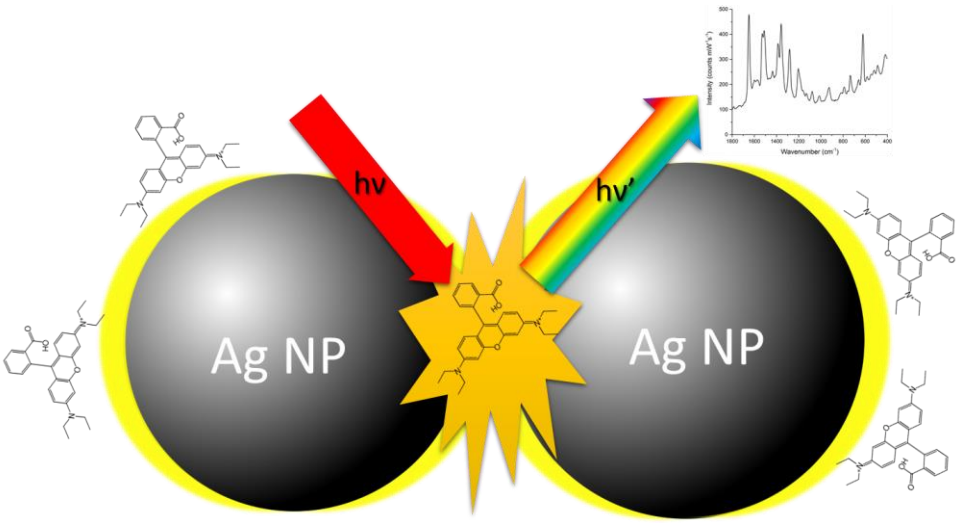

Figure 3. The hot spot is created when the chemisorbed analyte is localized in the high local field between silver nanoparticles during laser excitation.

SERS, like normal Raman, is a vibrational spectroscopy technique relying on the polarizability of a molecule to measure characteristic vibrational modes. However, SERS has the power to overcome challenges of Raman scattering and is ultrasensitive to the level of single molecules.[13,14] This minimally-invasive technique benefits from enhancement due to the intrinsic optical properties of the surface of noble metal nanoparticles and nanostructures. SERS has advanced into a sensitive analytical tool for the qualitative and quantitative detection of molecules adsorbed on nanostructures. Surface modification techniques have also allowed for improved analyte selectivity, including functionalization. SERS has advanced

to probe chemical queries in areas as diverse as chemistry, materials science, nanoscience and beyond.

References

1. McCreery, R. L. Raman Spectroscopy for Chemical Analysis. *Measurement Science and Technology* **2001***, 12*, 653.
2. Fleischmann, M.; Hendra, P. J.; McQuillan, A. J. Raman spectra of pyridine adsorbed at a silver electrode. *Chem. Phys. Lett.* **1974***, 26*, 163-166.
3. Jeanmaire, D. Surface Raman spectroelectrochemistry Part I. Heterocyclic, aromatic, and aliphatic amines adsorbed on the anodized silver electrode. *J. Electroanal. Chem.* **1977***, 84*, 1-20.
4. Albrecht, M. G.; Creighton, J. A. Anomalously intense Raman spectra of pyridine at a silver electrode. *J. Am. Chem. Soc.* **1977***, 99*, 5215-5217.
5. Stiles, P. L.; Dieringer, J. A.; Shah, N. C.; Van Duyne, R. P. Surface-Enhanced Raman Spectroscopy. *Annu. Rev. Anal. Chem.* **2008***, 1*, 601-626.
6. Shahbazyan, T.; Pustovit, V. Fluorescence quenching near small metal nanoparticles. *J. Chem. Phys.* **2012***, 136*, 6.
7. Kosuda, K. M.; Bingham, J. M.; Wustholz, K. L.; Van Duyne, R. P. Nanostructures and Surface-Enhanced Raman Spectroscopy. In *Comprehensive Nanoscience and Technology*; Andrews, D., Scholes, G. and Wiederrecht, G., Eds.; Academic Press: Oxford, 2011; pp 263-301.
8. Schatz, G. C.; Van Duyne, R. P.; Griffiths, P. R. Electromagnetic Mechanism of Surface-Enhanced Spectroscopy. In *Handbook of Vibrational Spectroscopy*; Chalmers, J. M., Griffiths, P. R., Eds.; Wiley & Sons: Chichester, UK, 2006; Vol. 1, pp 11-21.
9. Graham, D.; Faulds, K.; Smith, W. E. Biosensing using silver nanoparticles and surface enhanced resonance Raman scattering. *Chem. Commun.* **2006**, 4363-4371.
10. Lee, P. C.; Meisel, D. Adsorption and surface-enhanced Raman of dyes on silver and gold sols. *J. Phys. Chem.* **1982**, 3391-3395.
11. Shiohara, A.; Wang, Y.; Liz-Marzán, L. M. Recent approaches toward creation of hot spots for SERS detection. *J. Photochem. Photobiol., C* **2014***, 21*, 2-25.
12. Wustholz, K. L.; Henry, A.; McMahon, J. M.; Freeman, R. G.; Valley, N.; Piotti, M. E.; Natan, M. J.; Schatz, G. C.; Van Duyne, R. P. Structure-activity relationships in gold nanoparticle dimers and trimers for surface-enhanced Raman spectroscopy. *J. Am. Chem. Soc.* **2010***, 132*, 10903-10910.
13. Kleinman, S. L.; Ringe, E.; Valley, N.; Wustholz, K. L.; Phillips, E.; Scheidt, K. A.; Schatz, G. C.; Van Duyne, R.,P. Single-molecule surface-enhanced Raman spectroscopy of crystal violet isotopologues: theory and experiment. *J. Am. Chem. Soc.* **2011***, 133*, 4115.

14. Kneipp, K.; Wang, Y.; Kneipp, H.; Perelman, L. T.; Itzkan, I.; Dasari, R. R.; Feld, M. S. Single Molecule Detection Using Surface-Enhanced Raman Scattering (SERS). *Phys. Rev. Lett.* **1997***, 78*, 1667-1670.

Chapter 2: Research with Undergraduates at the Intersection of Chemistry and Art: Surface-Enhanced Raman Scattering Studies of Oil Paintings

Introduction

Undergraduate students are increasingly provided the opportunity to explore Raman spectroscopy as a part of their physical and analytical chemistry courses. Here, we describe a new approach for engaging undergraduate students with Raman spectroscopy in the research lab setting. In particular, Wustholz at William & Mary and Svoboda at Colonial Williamsburg engage in productive collaboration wherein predominately undergraduate students develop SERS-based methods to identify fugitive pigments in works of art. In this chapter, we describe several case studies that highlight the pedagogical journeys of student researchers working at the intersection of chemistry and art. We describe how this collaborative SERS research has led to discovery, innovation, and the professional development of undergraduates.

Our Story: Where Chemistry and Art Meet

Located in historic Williamsburg, Virginia, William & Mary is the second oldest college in the United States. Here, a diverse group of talented undergraduate students focusing on majors in the social sciences, humanities, and natural sciences converge to study and conduct research on shared curiosities. Since 2010, we have been interested in pursuing research with undergraduates at the intersection of chemistry and art. In particular, we

use surface-enhanced Raman scattering (SERS) spectroscopy to identify artists' pigments in historic paintings (Figure 1). This collaborative research has benefitted undergraduate students in several ways. First, SERS studies of art objects are an attractive way to introduce undergraduates to concepts in Raman spectroscopy and to develop their associated laboratory skills. Next, since undergraduates are inherently excited about research with real-world application, this project has been an effective tool to recruit students, particularly those from underrepresented groups, into the research lab. Finally, the students involved in this collaboration are productive and well prepared for future careers in chemistry. In this chapter, we present a series of colorful case studies, wherein former and current undergraduate researchers develop new methods for SERS-based analysis of art.

Figure 1. Lindsay Oakley (’12) prepares an art sample for SERS analysis with Wustholz in the paintings conservation lab of Colonial Williamsburg. Image courtesy of the Colonial Williamsburg Foundation.

Background: SERS in Conservation Science

The fading of colors in works of art is a major challenge for the conservation of our cultural heritage. As these "fugitive" colorants fade upon exposure to light, the aesthetics of the composition as well as the original intention of the artist can be significantly modified. In general, organic colorants are more susceptible to fading than their inorganic counterparts because of photo-oxidation and photo-induced dissociation of carbon-carbon bonds to produce a loss of color.[1] Figure 2 shows the chemical structures of several organic chromophores that comprise important fugitive artists' pigments. For conservation professionals, identifying fugitive, organic pigments in art is vital to understanding material degradation, identifying early stages of deterioration, and formulating more-informed exhibition guidelines. Unfortunately, however, the identification of organic dyes and pigments in art is one of the most significant challenges in conservation.

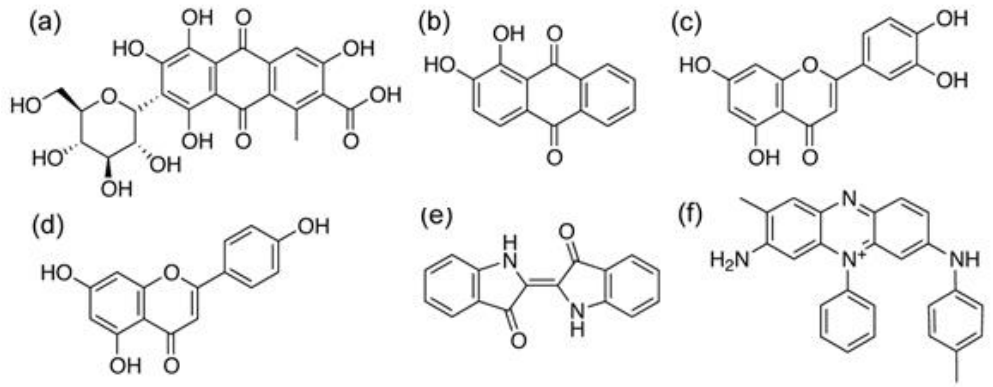

Figure 2. Chemical structures of the main component(s) of (a) carmine lake (carminic acid), (b) madder lake (alizarin), (c)-(d) Reseda lake (luteolin and apigenin, respectively), (e) indigo, and (f) mauve dye (mauveine A).

Conventional analytical techniques such as high performance liquid chromatography (HPLC) have been used to identify organic colorants, but require large samples (~1 mg) from a precious work of art, which are then destroyed in the analysis process.[2-4] Scanning electron microscopy with energy dispersive X-ray (SEM/EDX) is widely used in the conservation setting to perform elemental analysis.[5-8] However, this approach is limited to the detection of heavy atoms and does not provide for the identification of organic-based colorants. Raman spectroscopy can measure the unique vibrational signature of inorganic colorants such as vermilion, an important red inorganic pigment from the mineral cinnabar (Figure 3a). Yet, for most organic colorants (e.g., the red lake pigments carmine and madder lake), their weak Raman scattering signal is overwhelmed by molecular fluorescence.

To circumvent these issues, SERS spectroscopy is increasingly applied to the identification of organic colorants in art.[9-16] The noble-metal SERS substrate not only provides enhanced Raman scattering signals such that minute sample sizes (i.e., ~ng) are measurable, but also quenches the fluorescence generated by many organic colorants (Figure 3b). For example, Brosseau et al. applied SERS to the detection of fugitive red lake pigments in microscopic samples from pastels, watercolors, and textiles.[10,12] Owing to the remarkable signal enhancements in SERS, which can be up to ~10^{14} as compared to normal Raman scattering, considerable effort has been devoted

to understanding the underlying enhancement mechanisms.[17-21] In general, there is broad consensus that SERS studies of chromophores benefit significantly from the electromagnetic mechanism (EM) as well as resonance Raman effects.[19-22]

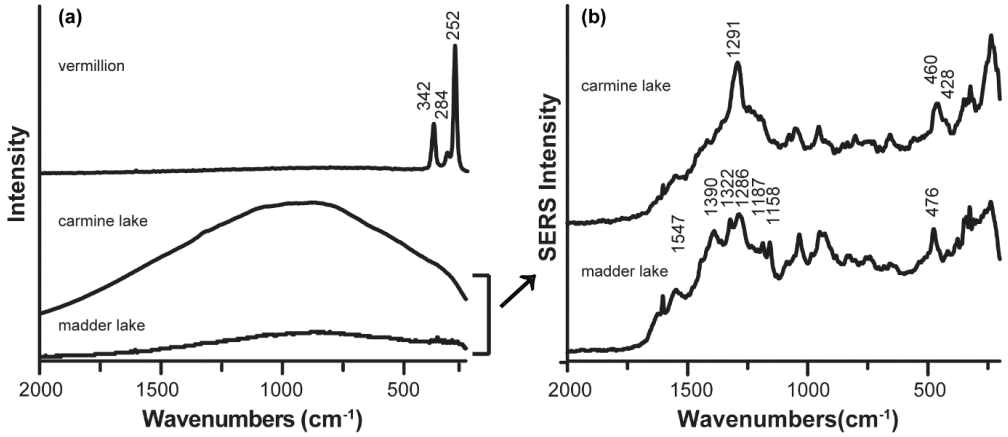

Figure 3. The normal Raman spectrum of vermilion is readily obtained using 785-nm excitation, but molecular fluorescence precludes Raman measurements of organic pigments carmine and madder lake. (b) Corresponding SERS spectra of the lake pigments obtained using citrate-reduced silver nanoparticles (AgNPs) as the enhancing substrate. Adapted with permission from reference 23. Copyright 2015 American Chemical Society.

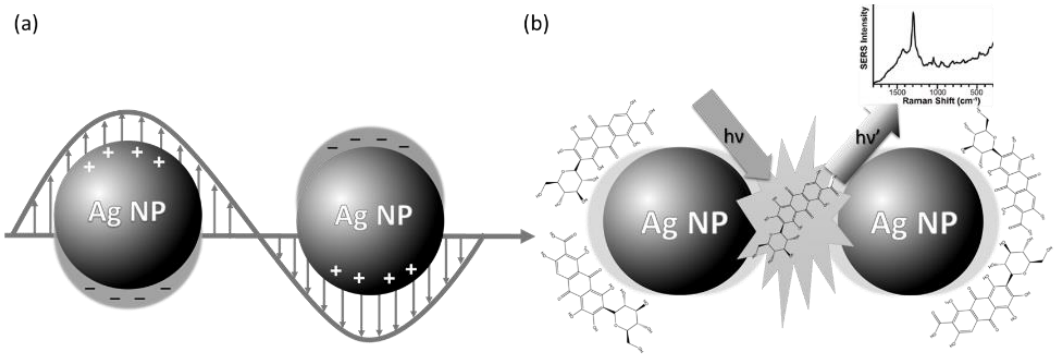

Figure 4. Schematic diagram of (a) a LSPR and (b) laser excitation of an organic chromophore (i.e., carminic acid) in an electromagnetic "hot spot" on the surface of AgNPs to produce SERS signal.

The EM is enhancement in the local field intensity as a result of excitation of a localized surface plasmon resonance (LSPR).[19,20,24] Figure 4 presents a schematic of how the incident electromagnetic field excites a collective oscillation of the conduction electrons in a noble metal nanoparticle, which results in enhanced fields close to the surface.[24] In particular, for a small metal sphere, the EM field intensity at the nanoparticle surface is given by: $|E_{out}|^2 = 2E_0^2|(\varepsilon_{in} - \varepsilon_{out})/(\varepsilon_{in} + 2\varepsilon_{out})|^2$, where ε_{in} and ε_{out} are the dielectric constants of the metal nanoparticle and external environment, respectively.[24] Maximum enhancement occurs when $\varepsilon_{in} \approx -2\varepsilon_{out}$, a resonance condition that is satisfied in the visible region for Au and Ag. Therefore, when an analyte (e.g., carminic acid – the primary component of carmine lake) is localized in a region of high EM enhancement such as a "hot spot,"[19,22,24] laser excitation of the sample yields extremely enhanced Raman signals (i.e., SERS). The extent of signal enhancement relative to normal Raman measurements is expressed as an enhancement factor (*EF*) that is given by:

$$EF = \frac{I_{SERS}/N_{SERS}}{I_{NRS}/N_{NRS}} \quad (1)$$

where I_{SERS} and I_{NRS} are the SERS and normal Raman scattering intensities, respectively, which are normalized by the number of molecules (*N*). Several groups have examined the SERS enhancement mechanism[17-21] and demonstrated the widespread applicability of SERS to problems in chemical and biological sensing.[25-32] For example, recent reviews have demonstrated

the application of SERS to the identification of colorants that are relevant to art and archaeology.[33-35]

Our research focuses on the development of SERS methodologies for the identification of fugitive organic pigments in oil paintings. Historic oil paintings may contain an amalgamation of colorants, resins, oils, gums, and waxes, all of which have undergone ageing and degradation. This inherent complexity represents a compelling real-world problem for undergraduate research students. How can SERS be used to identify the fugitive colorant within a microscopic paint sample, which can exhibit seemingly infinite spatial and temporal complexity? The following case studies highlight how undergraduate research in SERS can lead to discovery and innovation in both chemistry and art conservation as well as contribute to students' professional development.

Case Studies

Revealing Reds with Undergraduates

Due to the inherent complexity of historic oil paintings, organic pigments are typically extracted from the paint matrix, both mechanically and chemically, prior to investigation using SERS. For example, Leona and coworkers demonstrated the first SERS study of oil glazes, wherein hydrofluoric acid was used to pretreat disperse samples containing red lake pigments in order to

extract the colorant from the binding medium.[11,15] In this method, the acid pretreatment serves to hydrolyze the water-soluble dye from the insoluble lake pigment (e.g., carminic acid from carmine lake).[15] Although this approach is effective, a direct analysis of art samples without HF is preferable in the undergraduate research setting. In particular, a direct, non-hydrolysis approach has the advantages of preserving sample integrity, simplifying the analysis procedure, and most importantly, eliminating the hazards associated with using HF. Therefore, our first undergraduate research students, Lindsay Oakley (‘12) and Stephen Dinehart (‘12), set out to develop a non-hydrolysis SERS-based method for identifying fugitive red lake pigments in historic oil paintings.

Previous work by Brosseau and coworkers demonstrated that citrate-reduced silver nanoparticles (AgNPs)[36] are effective SERS substrates for identifying red lake pigments in relatively homogeneous artists’ media (i.e., pastels and watercolors).[12] As a first step toward non-hydrolysis SERS of oil paintings, the students made oil paints using historic methods and red lake pigments derived from the natural dyestuffs madder root, brazilwood, cinnabar, lac and cochineal insects. We demonstrated that AgNPs provide for the SERS-based identification of red lake pigments in reference paints.[37] Students also reported that understanding the origins of these colorants and making oil paints in the conservation setting are particularly appealing aspects of this project.

After these control experiments, Oakley traveled to the paintings conservation lab at nearby Colonial Williamsburg to meet her subjects, *Portrait of Isaac*

Barré by Sir Joshua Reynolds, 1766, and a painting by the earliest native-born American of European descent, *Portrait of William Nelson* by Robert Feke, circa 1750. Figure 5a shows the latter painting, which during conservation treatment exhibited some signs of minor fading. Working with a microscope and surgical blade, Svoboda performed the delicate work of removing a single pigment grain from the paint matrix of the faded region.

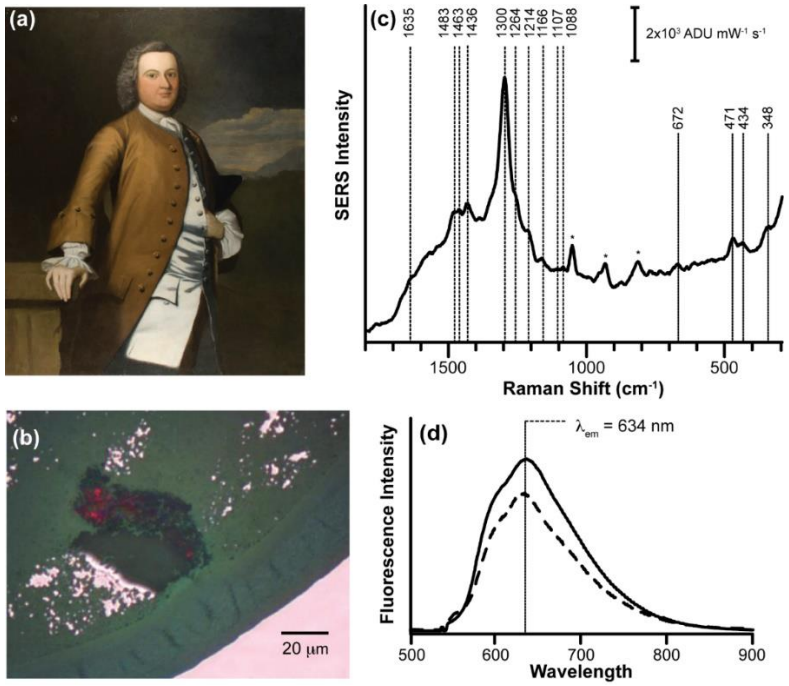

Figure 5. (a) Portrait of William Nelson *by Robert Feke, probably 1748-1750, CWF 1986-245. (b) Photomicrograph of lip sample coated in AgNPs. (c) Corresponding SERS spectrum obtained at 632.8-nm. Labeled peaks are consistent with carmine lake and asterisks denote bands due to adsorbed citrate. (d) Fluorescence spectra of the (solid line) lip sample) and a (dashed line) reference paint of carmine lake in linseed oil. Reproduced with permission from reference 37. Copyright 2011 American Chemical Society.*

Figure 5b shows a photomicrograph of sample obtained from the lip region of the *Portrait of William Nelson* and coated in AgNPs. Figure 5c presents the

SERS spectrum of the sample obtained using a Raman microscope with 632.8-nm excitation, with labeled peaks consistent with carmine lake.[37]

During the course of these studies, we observed that the AgNPs are not entirely adhered to the paint sample, since some regions of the sample exhibited excellent SERS signal while others produced solely fluorescence. Whereas SERS elucidates the vibrational fingerprint of an analyte, corresponding fluorescence measurements can provide a probe of local environment. For example, the fluorescence spectrum of the lip sample (Figure 5d) is an excellent match to a reference paint comprised of carmine lake in linseed oil. SERS measurements also revealed that Sir Joshua Reynolds used carmine lake to create the fleshtones in *Portrait of Isaac Barré*.[37] Corresponding fluorescence measurements support the interpretation that the binding medium for Reynolds' work contains both linseed oil and copal resin.

Ultimately, this correlated non-hydrolysis SERS and fluorescence approach enabled the definitive identification of the organic colorant and binding medium in an exceptionally small art sample, without the need for HF extraction. Moreover, this study demonstrated the utility of SERS for identifying red lake pigments in fleshtones – challenging regions that contain miniscule quantities of the sought colorant. Although this approach is effective for historic red lake pigments, we quickly discovered that the detection of yellow and blue organic pigments requires sample pretreatment. For example, Oakley worked with David Fabian (‘13) and Hannah Mayhew (‘14) to develop a simple, rapid

and effective protocol for SERS-based identification of indigo in microscopic paint from art.[38] In this approach, a sample pretreatment strategy based on the *in situ* conversion of insoluble indigo to soluble indigo carmine using H_2SO_4 is used to solubilize the pigment into the aqueous suspension of AgNPs. This study laid the groundwork for our growing interest in determining a general strategy to identify paint samples that contain pigment mixtures (e.g., optical mixtures of blue and yellow organic pigments that are used to create green paint).

It's Not Easy Being Green

An ideal analytical method for identifying pigments in historic oil paintings should be exceedingly sensitive, selective, minimally invasive, and applicable to a wide range of colorants. Although previous work by our group[37-40] and others[11,14,15] demonstrated the utility of SERS for identifying individual organic pigments in minute samples from historic oil paintings, none provided for the identification of pigment mixtures in paint. Considering the variety of colorants that are likely to appear in historic oil paint,[41] we decided to pursue a strategic approach for SERS-based analysis of pigment mixtures. In particular, motivated by the problem of fading in paint containing yellow organic pigments (e.g., green foliage that now appears blue), we investigated a series of green paints comprised of optical mixtures of blue and yellow organic pigments.

Joo Yeon (Diana) Roh (‘16) and Mary Matecki (‘16) first contributed to studying yellow organic pigments (i.e., Reseda lake, Stil de Grain, and gamboge) in reference samples of yellow and green paint.[40] Next, using a series of green reference paints, they established a practical flowchart for SERS-based identification of both the blue and yellow organic pigments within the paints.[41] In the first step, users obtain a normal Raman measurement of the untreated art sample to reveal the possible presence of the inorganic pigment, Prussian blue. If, however, the characteristic Raman bands for Prussian blue are not present and broad fluorescence band is observed, then sample treatment with HCl/MeOH is performed.[40]

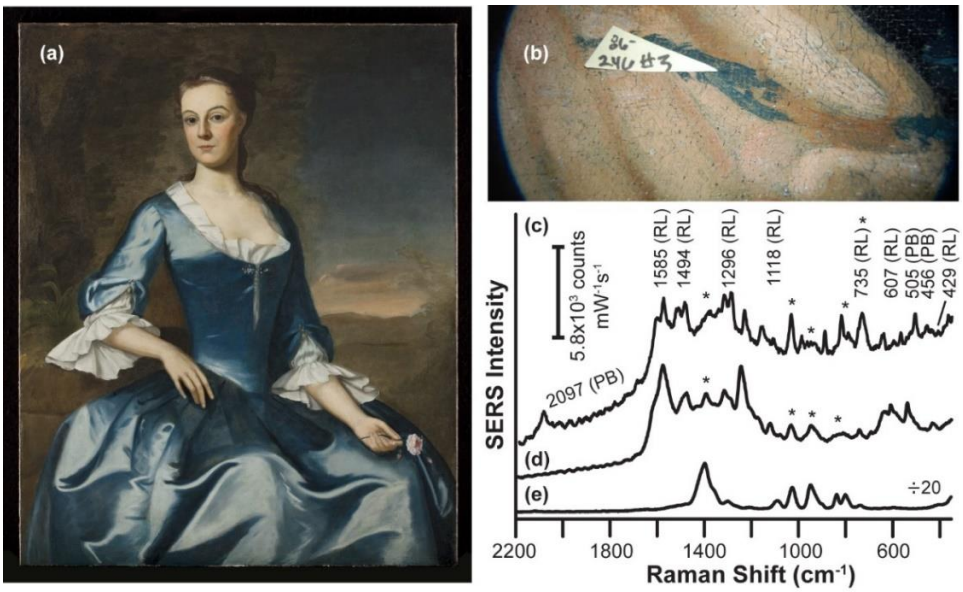

Figure 6. (a) Portrait of Elizabeth Burwell Nelson (Mrs. William Nelson) *by Robert Feke, probably 1748-1750, CWF 1986-246. (b) Photomicrograph of the rose stem where the microscopic sample was obtained. Corresponding SERS spectra of the sample obtained following the flowchart (c) after treatment with HCl/MeOH is compared to (d) reference green paint containing Reseda lake. Asterisks denote bands due to citrate. Reproduced with permission from reference* 41*. Copyright 2016 American Chemical Society.*

If, on the other hand, weak Raman scattering at ~1633 and ~1592 cm^{-1} are observed, consistent with gamboge, users perform an extraction step with acetonitrile and water. After SERS measurements to reveal the yellow, organic pigment, the final step is to treat the sample with H_2SO_4 to elucidate indigo using SERS.

After success with the reference samples, Roh and Matecki subjected the flowchart approach to the ultimate challenge – a minute sample from the *Portrait of Elizabeth Burwell Nelson (Mrs. William Nelson)* by Robert Feke (Figure 6a). In this portrait, the sitter holds a rose stem that now appears blue (Figure 6b), suggesting the presence of a photosensitive yellow organic pigment that has faded over time. To test this hypothesis, we examined a microscopic sample from the stem following the treatment flowchart. At step 1, the sample exhibited normal Raman peaks due to Prussian blue (PB), with no evidence for gamboge. Therefore, the sample was treated with HCl/MeOH to reveal SERS bands at 1585, 1494, 1296, 1118, 735, 607, and 429 cm^{-1} for Reseda lake (RL), as shown in Figure 6c. This study marked the first successful identification of a yellow lake pigment in a historic painting and the first detection of two different pigments in a single paint sample.[41]

SERS Analysis of Early Work by Paul Cézanne

Although SERS studies of oil paintings have demonstrated high sensitivity and selectivity, these investigations are largely focused on natural,

organic colorants that originate from plant and animal sources. To extend the applicability of SERS to a wider range of organic colorants, we turned our attention to the early, synthetic dyes that date to the mid-19th century. In particular, Kristen Frano (M.S. '15) used SERS to examine the first synthetic organic dye, mauve, which was serendipitously discovered by William Henry Perkin in 1856.[42,43]

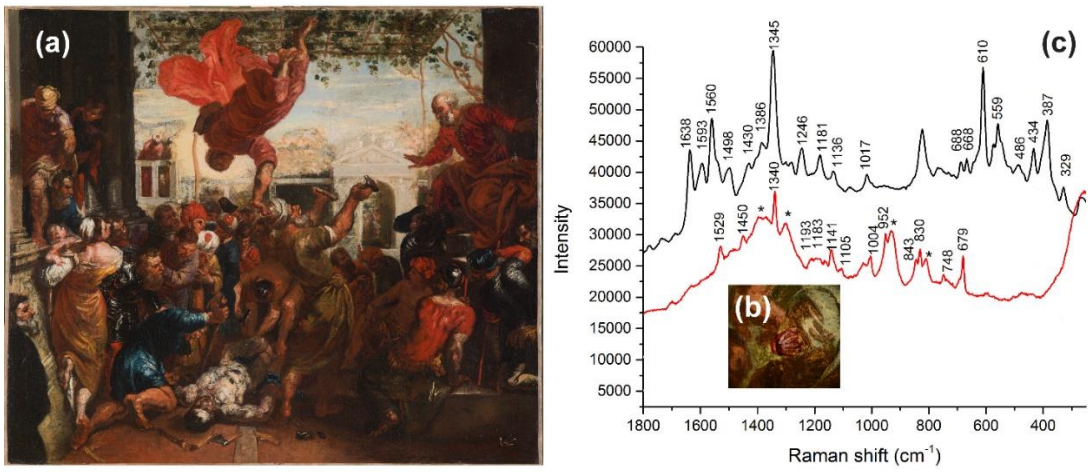

Figure 7. (a) Miracle of the Slave, Paul Cézanne after Jacopo Tintoretto, c. 1856-1870, Muscarelle Museum of Art, 2014.067. (b) Photomicrograph of red-violet turban detail. (c) Corresponding SERS spectra of the (red line) sample and (black line) reference mauve dye from a modern synthesis, obtained using 632.8-nm excitation. Asterisks denote bands due to citrate. Images courtesy of the Muscarelle Museum of Art at the College of William and Mary, Williamsburg, VA.

Previous work by Cañamares and coworkers[44,45] demonstrated that coupling thin layer chromatography to SERS provides for structural elucidation of the main components in mauve dye. However, to our knowledge, mauve dye had not been identified in an actual work of art.

Miracle of the Slave, a recent acquisition by the Muscarelle Museum of Art at William & Mary, provided an interesting case study for our research group. Visual inspection of the painting by a team of curators indicated that *Miracle of the Slave* (Figure 7a) was painted by Paul Cézanne as a copy of an original work by Jacopo "Tintoretto" Robusti. To examine this hypothesis, we examined the luminous regions of transparent paint, which are consistent with the presence of organic dye-based colors, using direct, non-hydrolysis SERS.[37] SERS spectra of the red-violet hues found in the turban details of the figure just left of center (Figure 7b), obtained using 632.8-nm excitation, are inconsistent with references for a variety of modern and historic red and purple colorants (i.e., madder lake, carmine lake, lac, brazilwood, logwood, Tyrian purple, kermes, crystal violet, cobalt violet, rhodamine B, dioxazine violet). The observed SERS peaks at 1529, 1450, 1340, 1193, 1183, 1141, 1105, 1004, 952, 843, 830, 748, and 679 cm^{-1} are consistent with reference samples of mauve dye prepared using a modern synthesis.[44-46] However, several prominent vibrational modes for the modern mauve dye (i.e., 1638, 1593, 1560, 610, 559, 434, and 387 cm^{-1}) are absent from the art sample.[45,47] It is possible that degradation of the historical sample as well as a difference in chromophore composition between the modern synthesis and a period synthesis prepared from coal tar explain these discrepancies.

Ultimately, based on the observed SERS spectral correlation to mauve and the lack of evidence for alternative colorants, the red-violet hue in the

turban is attributed to an early synthetic organic colorant, most likely mauve or analogous aniline derivative. With its intense color and low cost, mauve became extremely popular very quickly and Perkins' establishment of a factory in 1862 to produce mauve commercially marked the beginning of the modern dye industry.[42,43] Its presence in *Miracle of the Slave* firmly refines the date of the painting to a time after 1856, consistent with the initial attribution of the painting to the early period of Paul Cézanne.

Engaging Undergraduates with SERS in Teaching Labs

The undergraduate students involved in SERS studies of art are exceedingly enthusiastic about their research and eager to share their results with others. This enthusiasm inspired us to develop a new experiment for an upper-division teaching laboratory that simulates a problem-solving scenario in the conservation setting. In particular, students enrolled in the *Integrated Physical and Analytical Chemistry Laboratory* are challenged to identify the pigments in a mock Warhol-inspired oil painting. Although several laboratory experiments to explore SERS[44-47] and the field of art conservation[48-51] existed, none integrated SERS with art conservation. Frano and Mayhew developed a problem-based learning approach to the experiment, where the instructor facilitates group discussion and guides student inquiry to solve the problem – in this case, identifying unknown pigments in a "precious" artwork.[23]

Students begin by evaluating the different analytical techniques that might be appropriate for painting analysis. After determining that Raman spectroscopy is a reasonable approach for this purpose, students attempt normal Raman measurements on the painting (Figure 8), which is comprised of inorganic (nonfluorescent) and organic (fluorescent) pigments.

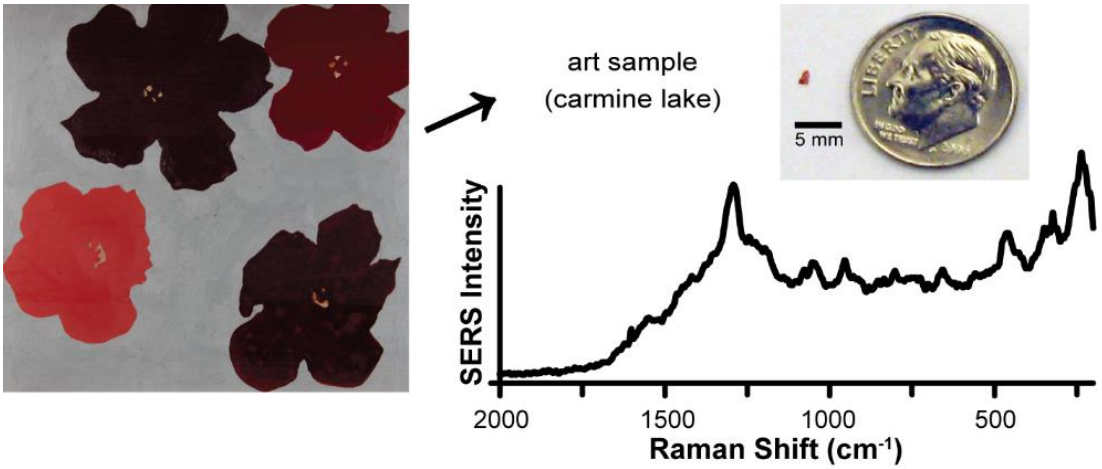

Figure 8. Schematic of the procedure for an upper-division laboratory experiment where students analyze minute samples from an oil painting using a benchtop Raman spectrometer equipped with 785-nm laser excitation. Adapted with permission from reference 23. Copyright 2015 American Chemical Society.

When confronted with the broad, featureless spectra of the organic pigments, students proceed to synthesize AgNPs for SERS analysis and extract a microscopic sample from the painting using a surgical blade.[36] To date, approximately 200 students have conducted this experiment and successfully identified vermilion, lac dye, carmine lake, and madder lake paints. According to student feedback, one of the strongest aspects of the experiment is problem solving a real-world investigation from beginning to end.[9]

More recently, Wustholz has developed a course for first-year undergraduate students, *Light at the Museum: the Science and Art of Conservation*. In this course, undergraduates learn how scientists use techniques such as Raman spectroscopy and SERS to identify artists' materials in actual works of art. The learning outcomes for this class are evaluated using a series of scaffolded assignments, where students build the knowledge and skills necessary to create a presentation to the class on a museum object. In the final presentation, students explain, interpret, and analyze the results of a technical examination and their bearing on the artwork itself (e.g., historical significance, artist, attribution, conservation). We find that art conservation is an appealing vehicle through which to deliver fundamental concepts in Raman spectroscopy.

Conclusion: Where Are They Now?

Where are they – the paintings and the students – now? The information revealed by our SERS analyses of paintings is often presented to museum visitors in the form of digital reconstructions. These reconstructions, informed by chemical characterization performed by undergraduate students, offer insight into the original intent of the artist before fading occurred. Ultimately, the definitive identification of the more vulnerable organic-based colors so sought after by artists helps the viewer – curator, conservator, chemist, museum-goer

– better understand their original appearances as well as color changes as part of the patina of age.

Since 2010, 14 students have been involved this collaboration, including 12 women and another 2 from underrepresented groups. Of these 14 students, 8 have co-authored manuscripts, 6 have gone on to Ph.D. programs in chemistry or materials science, and the rest to medicine, education, or industry positions. Interestingly, most of the undergraduate research students who went to Ph.D. programs were initially planning other careers. For example, Lindsay Oakley ('12) originally stated that she wasn't interested in graduate school in chemistry but that she loved art history. Just two years later, she had discovered a passion for research, co-authored two manuscripts, and was headed to a top Ph.D. program in materials science and engineering at Northwestern University. She recently obtained a Ph.D. and is currently focusing on conservation research in Denmark. Other former undergraduate researchers like Fabian, Roh, and Choffel, and are pursuing graduate-level research in chemistry.

Engaging students in SERS research through the lens of art conservation exposes bright minds to opportunities outside of the standard chemistry curricula. As they gain experience handling minute samples from precious paintings and working in the conservation setting, students develop excellent problem-solving, hand, and communication skills. Ultimately, these SERS-based research and teaching experiences are an effective way to

enhance the preparation of undergraduate students for future careers in chemistry as part of a robust liberal arts education.

Acknowledgments

We gratefully and wholeheartedly thank the former and current students that have driven this collaborative research project: Lindsay Oakley, Stephen Dinehart, David Fabian, Hannah Mayhew, Kristen Frano, Diana Roh, Mary Matecki, Kathleen Nelsen, Marisa Choffel, Carolyn Farling, Kalie Fikse, and Kathleen Lauer. We acknowledge the Eppley Foundation for Research, Jeffress Memorial Trust, and the William & Mary Charles Center for funding of this project. We are also indebted to Colonial Williamsburg for continued support of this collaboration and especially to Ronald L. Hurst, Vice President for Collections, Conservation, and Museums and The Carlisle H. Humelsine Chief Curator at Colonial Williamsburg Foundation.

References

1. Oda, H. An approach to the photostabilization of dyes: the effect of UV absorbers containing a built-in photostabilizer moiety on the light fastness of acid dyes. *Dyes Pigm.* **2001***, 48*, 151-157.
2. Karapanagiotis, I.; Valianou, L.; Daniilia, S.; Chryssoulakis, Y. Organic dyes in Byzantine and post-Byzantine icons from Chalkidiki (Greece). *J. Cult. Herit.* **2007***, 8*, 294-298.
3. Novotná, P.; Pacáková, V.; Bosáková, Z.; Štulík, K. High-performance liquid chromatographic determination of some anthraquinone and naphthoquinone dyes occurring in historical textiles. *J. Chromatogr. A* **1999***, 863*, 235-241.
4. van Bommel, M. R.; Berghe, I. V.; Wallert, A. M.; Boitelle, R.; Wouters, J. High-performance liquid chromatography and non-destructive three-dimensional fluorescence analysis of early synthetic dyes. *J. Chromatogr. A* **2007***, 1157*, 260-272.
5. Boon, J. J.; Keune, K.; van der Weerd, J.; Geldof, M.; van Asperen de Boer, J R J Imaging Microspectroscopic, Secondary Ion Mass Spectrometric and Electron Microscopic Studies on Discoloured and Partially Discoloured Smalt in Cross-sections of 16th Century Paintings. *CHIMIA* **2001***, 55*, 952-960.
6. Rampazzi, L.; Cariati, F.; Tanda, G.; Colombini, M. P. Characterisation of wall paintings in the Sos Furrighesos necropolis (Anela, Italy). *J. Cult. Herit.* **2002***, 3*, 237-240.
7. Andreotti, A.; Colombini, M. P.; Nevin, A.; Melessanaki, K.; Pouli, P.; Fotakis, C. Multianalytical Study of Laser Pulse Duration Effects in the IR Laser Cleaning of Wall Paintings from the Monumental Cemetery of Pisa. *Laser Chem.* **2006***, 2006*, 1-11.
8. Keune, K.; Mass, J.; Mehta, A.; Church, J.; Meirer, F. Analytical imaging studies of the migration of degraded orpiment, realgar, and emerald green pigments in historic paintings and related conservation issues. *Herit. Sci.* **2016***, 4*, 1-14.
9. Van Elslande, E.; Lecomte, S.; Le Hô, A. Micro-Raman spectroscopy (MRS) and surface-enhanced Raman scattering (SERS) on organic colourants in archaeological pigments. *J. Raman Spectrosc.* **2008***, 39*, 1001-1006.
10. Brosseau, C. L.; Casadio, F.; Van Duyne, R. P. Revealing the invisible: using surface-enhanced Raman spectroscopy to identify minute remnants

of color in Winslow Homer's colorless skies. *J. Raman Spectrosc.* **2011***, 42*, 1305-1310.

11. Pozzi, F.; Lombardi, J. R.; Bruni, S.; Leona, M. Sample Treatment Considerations in the Analysis of Organic Colorants by Surface-Enhanced Raman Scattering. *Anal. Chem.* **2012***, 84*, 3751-3757.
12. Brosseau, C. L.; Rayner, K. S.; Casadio, F.; Grzywacz, C. M.; Van Duyne, R. P. Surface-Enhanced Raman Spectroscopy: A Direct Method to Identify Colorants in Various Artist Media. *Anal. Chem.* **2009***, 81*, 7443-7447.
13. Castro, R.; Pozzi, F.; Leona, M.; Melo, M. J. Combining SERS and microspectrofluorimetry with historically accurate reconstructions for the characterization of lac dye paints in medieval manuscript illuminations. *J. Raman Spectrosc.* **2014***, 45*, 1172-1179.
14. Pozzi, F.; Berg, K. J.; Fiedler, I.; Casadio, F. A systematic analysis of red lake pigments in French Impressionist and Post-Impressionist paintings by surface-enhanced Raman spectroscopy (SERS). *J. Raman Spectrosc.* **2014***, 45*, 1119-1126.
15. Leona, M.; Hoffmann, R. Microanalysis of Organic Pigments and Glazes in Polychrome Works of Art by Surface-Enhanced Resonance Raman Scattering. *PNAS* **2009***, 106*, 14757-14762.
16. Van Elslande, E.; Lecomte, S.; Le Hô, A. Micro-Raman spectroscopy (MRS) and surface-enhanced Raman scattering (SERS) on organic colourants in archaeological pigments. *J. Raman Spectrosc.* **2008***, 39*, 1001-1006.
17. Kneipp, K.; Wang, Y.; Kneipp, H.; Perelman, L. T.; Itzkan, I.; Dasari, R. R.; Feld, M. S. Single Molecule Detection Using Surface-Enhanced Raman Scattering (SERS). *Phys. Rev. Lett.* **1997***, 78*, 1667-1670.
18. Dieringer, J. A.; Lettan, 2., Robert B; Scheidt, K. A.; Van Duyne, R. P. A frequency domain existence proof of single-molecule surface-enhanced Raman spectroscopy. *J. Am. Chem. Soc.* **2007***, 129*, 16249-16256.
19. Stiles, P. L.; Dieringer, J. A.; Shah, N. C.; Van Duyne, R. P. Surface-Enhanced Raman Spectroscopy. *Ann. Rev. Anal. Chem.* **2008***, 1*, 601-626.
20. Schatz, G. C.; Van Duyne, R. P.; Griffiths, P. R. Electromagnetic Mechanism of Surface-Enhanced Spectroscopy. In *Handbook of Vibrational Spectroscopy*; Chalmers, J. M., Griffiths, P. R., Eds.; Wiley & Sons: Chichester, UK, 2006; Vol. 1, pp 11-21.
21. Kleinman, S. L.; Ringe, E.; Valley, N.; Wustholz, K. L.; Phillips, E.; Scheidt, K. A.; Schatz, G. C.; Van Duyne, R. P. Single- molecule surface- enhanced

Raman spectroscopy of crystal violet isotopologues: theory and experiment. *J. Am. Chem. Soc.* **2011***, 133*, 4115.

22. Wustholz, K. L.; Henry, A.; McMahon, J. M.; Freeman, R. G.; Valley, N.; Piotti, M. E.; Natan, M. J.; Schatz, G. C.; Van Duyne, R. P. Structure-activity relationships in gold nanoparticle dimers and trimers for surface-enhanced Raman spectroscopy. *J. Am. Chem. Soc.* **2010***, 132*, 10903-10910.
23. Mayhew, H. E.; Frano, K. A.; Svoboda, S. A.; Wustholz, K. L. Using Raman spectroscopy and surface-enhanced Raman scattering to identify colorants in art: an experiment for an upper-division chemistry laboratory. *J. Chem. Educ.* **2015***, 92*, 148-152.
24. Kosuda, K. M.; Bingham, J. M.; Wustholz, K. L.; Van Duyne, R. P. Nanostructures and Surface-Enhanced Raman Spectroscopy. In *Comprehensive Nanoscience and Technology*; Andrews, D., Scholes, G. and Wiederrecht, G., Eds.; Academic Press: Oxford, 2011; pp 263-301.
25. Zaleski, S.; Cardinal, M. F.; Chulhai, D. V.; Wilson, A. J.; Willets, K. A.; Jensen, L.; Van Duyne, R. P. Toward Monitoring Electrochemical Reactions with Dual-Wavelength SERS: Characterization of Rhodamine 6G (R6G) Neutral Radical Species and Covalent Tethering of R6G to Silver Nanoparticles. *J. Phys. Chem.* **2016***, 120*, 24982-24991.
26. Kneipp, J.; Kneipp, H.; Wittig, B.; Kneipp, K. Following the Dynamics of pH in Endosomes of Live Cells with SERS Nanosensors. *J. Phys. Chem.* **2010***, 114*, 7421-7426.
27. Kneipp, J.; Kneipp, H.; Wittig, B.; Kneipp, K. One- and two-photon excited optical ph probing for cells using surface-enhanced Raman and hyper-Raman nanosensors. *Nano Lett.* **2007***, 7*, 2819-2823.
28. Bishnoi, S. W.; Rozell, C. J.; Levin, C. S.; Gheith, M. K.; Johnson, B. R.; Johnson, D. H.; Halas, N. J. All-optical nanoscale pH meter. *Nano Lett.* **2006***, 6*, 1687-1692.
29. Graham, D.; Faulds, K.; Smith, W. E. Biosensing using silver nanoparticles and surface enhanced resonance Raman scattering. *Chem. Commun.* **2006**, 4363-4371.
30. Taylor, J.; Huefner, A.; Li, L.; Wingfield, J.; Mahajan, S. Nanoparticles and intracellular applications of surface-enhanced Raman spectroscopy. *Analyst* **2016***, 141*, 5037-5055.
31. Piotrowski, P.; Wrzosek, B.; Królikowska, A.; Bukowska, J. A SERS-based pH sensor utilizing 3-amino-5-mercapto-1,2,4-triazole functionalized Ag nanoparticles. *Analyst* **2014***, 139*, 1101-1111.

32. Ngo, H. T.; Wang, H.; Fales, A. M.; Vo-Dinh, T. Plasmonic SERS biosensing nanochips for DNA detection. *Anal. Bioanal. Chem.* **2016***, 408*, 1773-1781.
33. Wustholz, K. L.; Brosseau, C. L.; Casadio, F.; Van Duyne, R. P. Surface-enhanced Raman spectroscopy of dyes: from single molecules to the artists' canvas. *Phys. Chem. Chem. Phys.* **2009***, 11*, 7350-7359.
34. Chen, K.; Leona, M.; Vo-Dinh, T. Surface-enhanced Raman scattering for identification of organic pigments and dyes in works of art and cultural heritage material. *Sens. Rev.* **2007***, 27*, 109-120.
35. Casadio, F.; Leona, M.; Lombardi, J. R.; Van Duyne, R. Identification of organic colorants in fibers, paints, and glazes by surface enhanced Raman spectroscopy. *Acc. Chem. Res.* **2010***, 43*, 782-791.
36. Lee, P. C.; Meisel, D. Adsorption and surface-enhanced Raman of dyes on silver and gold sols. *J. Phys. Chem.* **1982**, 3391-3395.
37. Oakley, L. H.; Dinehart, S. A.; Svoboda, S. A.; Wustholz, K. L. Identification of Organic Materials in Historic Oil Paintings Using Correlated Extractionless Surface-Enhanced Raman Scattering and Fluorescence Microscopy. *Anal. Chem.* **2011***, 83*, 3986-3989.
38. Oakley, L. H.; Fabian, D. M.; Mayhew, H. E.; Svoboda, S. A.; Wustholz, K. L. Pretreatment Strategies for SERS Analysis of Indigo and Prussian Blue in Aged Painted Surfaces. *Anal. Chem.* **2012***, 84*, 8006-8012.
39. Frano, K. A.; Mayhew, H. E.; Svoboda, S. A.; Wustholz, K. L. Combined SERS and Raman analysis for the identification of red pigments in cross-sections from historic oil paintings. *Analyst* **2014***, 139*, 6450-6455.
40. Mayhew, H. E.; Fabian, D. M.; Svoboda, S. A.; Wustholz, K. L. Surface-enhanced Raman spectroscopy studies of yellow organic dyestuffs and lake pigments in oil paint. *Analyst* **2013***, 138*, 4493-4499.
41. Roh, J. Y.; Matecki, M. K.; Svoboda, S. A.; Wustholz, K. L. Identifying Pigment Mixtures in Art Using SERS: A Treatment Flowchart Approach. *Anal. Chem.* **2016***, 88*, 2028-2032.
42. Sousa, M. M.; Melo, M. J.; Parola, A. J.; Morris, P. J. T.; Rzepa, H. S.; de Melo, J Sérgio Seixas A study in mauve: unveiling Perkin's dye in historic samples. *Chem. Eur. J.* **2008***, 14*, 8507-8513.
43. Conceição Oliveira, M. d.; Dias, A.; Douglas, P.; Seixas de Melo, J S Perkin’s and Caro’s Mauveine in Queen Victoria’s Lilac Postage Stamps: A Chemical Analysis. *Chem. Eur. J.* **2014***, 20*, 1808-1812.
44. Cañamares, M. V.; Reagan, D. A.; Lombardi, J. R.; Leona, M. TLC-SERS of mauve, the first synthetic dye. *J. Raman Spectrosc.* **2014***, 45*, 1147-1152.

45. Cañamares, M. V.; Lombardi, J. R. Raman, SERS, and DFT of Mauve Dye: Adsorption on Ag Nanoparticles. *J. Phys. Chem. C* **2015***, 119*, 14297-14303.
46. Scaccia, R. L.; Coughlin, D.; Ball, D. W. A microscale synthesis of mauve. *J. Chem. Educ.* **1998***, 75*, 769.
47. Galasso, V. A DFT characterization of the structures and UV/vis absorption spectra of mauveine dyes. *Chem. Phys. Lett.* **2008***, 457*, 250-253.
48. Nivens, D. A.; Padgett, C. W.; Chase, J. M.; Verges, K. J.; Jamieson, D. S. Art, Meet Chemistry; Chemistry, Meet Art: Case Studies, Current Literature, and Instrumental Methods Combined to Create a Hands-On Experience for Nonmajors and Instrumental Analysis Students. *J. Chem. Educ.* **2010***, 87*, 1089-1093.
49. Smith, G.; Nunan, E.; Walker, C.; Kushel, D. Inexpensive, Near-Infrared Imaging of Artwork Using a Night- Vision Webcam for Chemistry-of-Art Courses. *J. Chem. Educ.* **2009***, 86*, 1382-1388.
50. Harmon, K.; Miller, L.; Millard, J. Crime Scene Investigation in the Art World: The Case of the Missing Masterpiece. *J. Chem. Educ.* **2009***, 86*, 817-819.
51. Nielsen, S. E.; Scaffidi, J.; Yezierski, E. J. Detecting Art Forgeries: A Problem- Based Raman Spectroscopy Lab. *J. Chem. Educ.* **2014***, 91*, 446-450.

Chapter 3: SERS pH Sensing

SERS for Theranostics: Background

SERS has powerful capability as a diagnostic tool in various nanophotonics for theranostics including biosensing applications. Theranostics is the portmanteau term for an application that pursues new diagnostic and therapeutic measures to monitor and target disease.[1] To date, SERS has been applied to glucose sensing,[2-5] DNA detection,[6-9] and intracellular monitoring of drug effects.[10,11] Owing to its ultrasensitive and unambiguous reporting SERS has been applied in both solid- and solution-phase experiments. SERS substrate stability in aqueous suspensions also makes it an ideal technique in biological environments. Additionally, Raman measurements benefit from a wide spectral range due to its intrinsic scattering effect, which differs from other spectroscopic techniques requiring specific excitation and emission wavelengths for each particular analyte. However, SERS applications can also gain intensity by exciting at the particular resonance frequency of the analyte molecule to produce resonance Raman enhancement. Though SERS biosensors have gained momentum in recent years, major challenges still exist. For example, glucose exhibits small normal Raman cross-sections and weak adsorption to free SERS-active surfaces, such as roughened silver substrates have been observed.[3] However, the biological applications of SERS are increasingly moving forward to address real-world applications. For example, Kircher and colleagues improved tumor visualization via magnetic-resonance

and photoacoustic imaging combined with surface-enhanced Raman analysis to conduct *in vivo* tumor resection surgeries as successfully demonstrated in living mice.[12]

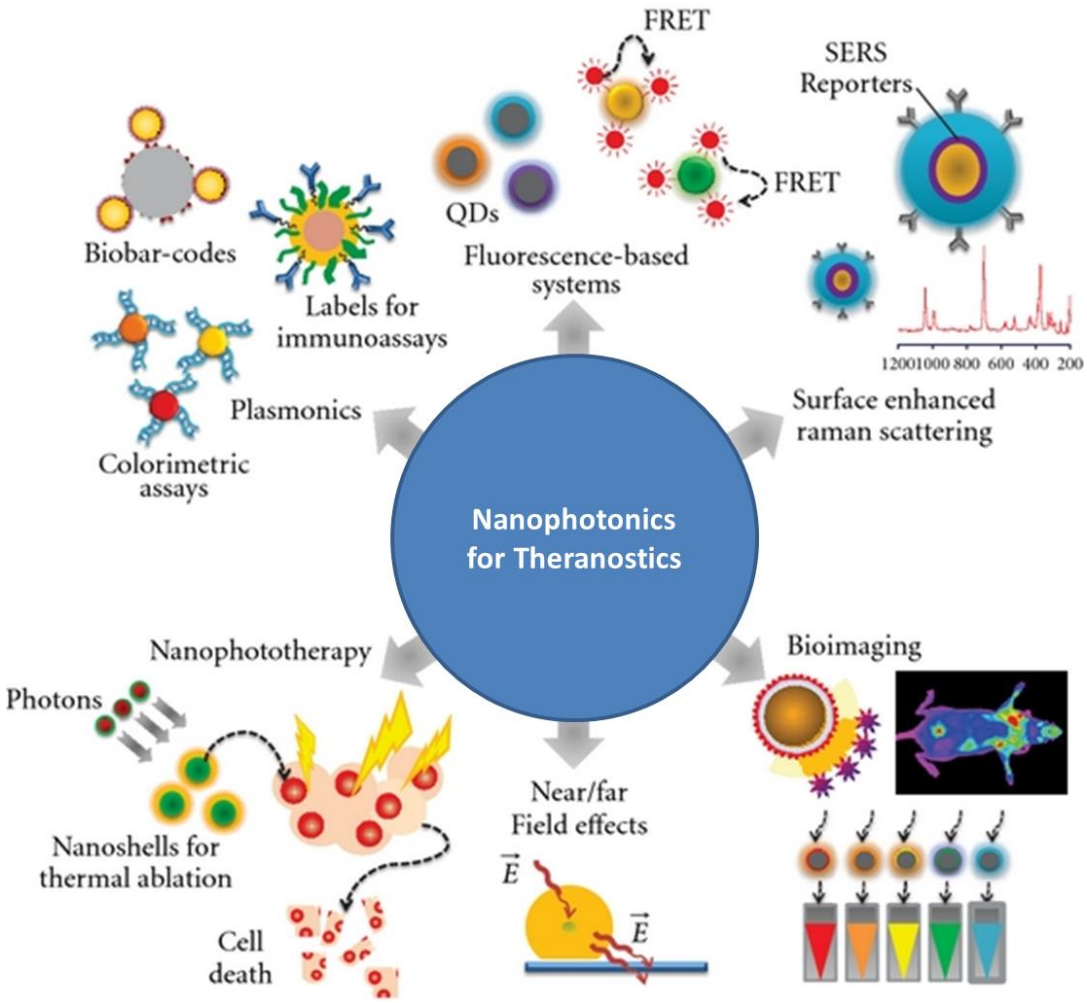

Figure 1. Schematic of various developing methods and applications in the field of nanotechnology theranostics. Adapted from reference 1.

Several groups have demonstrated the widespread applicability of SERS to problems in chemical and biological sensing.[13-20] For example, recent reviews

have explored SERS utility for diagnostics at the molecular level in biological[21,22] and environmental[23] assays.

Emerging biosensing techniques for mapping pH in cellular environments are complicated by the complex molecular matrix within cells. Tumor microenvironments are a topic of interest for many researchers because of the effects of changing local environments such as lowering of pH and increased temperature, which increase the spread of cancer cells.[24] Fluorescent dyes have been utilized to probe the pH of these complex environments but face further challenges due to the lack of photostability. Fluorescent dyes as molecular pH probes have been explored in several studies.[25-29] However, there is still a need for a method to probe pH in complex microenvironments with high sensitivity, selectivity and increased spatial resolution.

Surface-enhanced Raman spectroscopy is applied to address the issues faced by fluorescent pH probes. The SERS technique has an enhancement capability upwards of 10 orders of magnitude in a resonant system revealing characteristic chemical fingerprints of the analyte dye in condensed-phase experiments.[30] Bishnoi and coworkers used gold nanoparticles (AuNPs) to serve as optical pH sensors consisting Au nanoshell spheres and an adsorbed monolayer of para-mercaptobenzoic acid (pMBA).[16] However, this requires the use of additional steps to form the adsorbed pMBA

monolayer, which also shortens the shelf-life of the colloidal suspension due to increased aggregation and subsequent deactivation of the nanoparticles.

The purpose of the current study is to make a simple, stable, and sensitive SERS pH probe. For this goal, we utilized a pH-sensitive dye that is stable in an aqueous environment but did not require additional steps that would hinder particle stability. We enlisted the synthetic expertise of the Harbron group at William and Mary to supply the pH probe dye. Rhodamine spirolactam (RSL) dyes are fluorescent pH probes and tunable to target specific pK_a values by substituting functional groups on the spirolactam ring, e.g. 2,6-diisopropylaniline (RB-DIA) as shown in Figure 2. The functionalization of RSL dyes makes RSLs robust pH reporters.

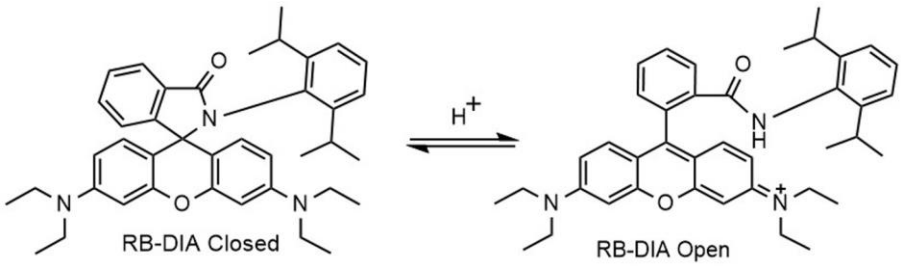

Figure 2. Rhodamine B-based spirolactam RSL dye for pH sensing.

As the proton concentration is increased in solution, the spirolactam ring opens and becomes abundantly more SERS active due to the increase in conjugation (Figure 2). In previous fluorescent pH probe work, the pK_a has been calculated based on sigmoidal curve fitting of fluorescence intensities as a response to

changing pH by applying a Henderson–Hasselbalch-style mass action equation, Equation 1.[31]

$$pK_a = pH - log\left(\frac{I_{max}-I}{I-I_{min}}\right) \quad (1)$$

The goals were to develop SERS-based strategies to address the complications of photostability and intensity in solution-phase pH sensing by optimizing SERS substrates, to evaluate p*K*a of the analyte dye, to explore electrostatic interactions, and to create a predictive model for SERS RSL pH probes.

Experimental

Substrate synthesis

Citrate-reduced silver nanoparticle (AgNP) substrates were prepared by the Lee-Meisel method.[32] Nanoparticle synthesis is a sensitive process that must be completed in clean glassware with surfaces appropriate for nanoparticle synthesis. To clean the glassware and stir bar, 80-mL of *aqua regia* (1:3 nitric acid and hydrochloric acid solution) was used to remove any residual metal. Afterwards, the glassware and stir bar are carefully rinsed with ultrapure water (MilliQ) to remove the excess *aqua regia*. The glassware was then placed in a base bath of 1 M KOH in 4:1 ethanol and water for 24 hours. Finally, the glassware and stir bar were rinsed thoroughly with ultrapure water. To begin

the AgNP synthesis, a 1000-mL Erlenmeyer flask containing 500-mL dd-H_2O MilliQ was heated with stiring. In darkened lab conditions, approximately 92.2 mg silver nitrate ($AgNO_3$) was added to heated water in the reaction vessel. After reaching a vigorous boil, 10-mL of a 1% (w/v) sodium citrate solution was added to the reaction vessel. After the characteristic color change from clear and colorless to clear and yellow to turbid and green is observed, the reaction vessel is heated for an additional 30 minutes or until approximately 275-mL of solution remains. To assess the quality of the AgNP synthesis, SERS intensity of the ~1400 cm^{-1} of the citrate capping agent was measured for wet 0.75-µL droplets on glass coverslips.

SERS measurements

All SERS measurements were conducted with an inverted confocal microscope (Nikon, TiU) with spectrograph (Princeton Instruments, SP2356, 600 g/mm grating) using excitation at 632.8-nm from a HeNe laser source (Research Electro-Optics). Each sample measurement was collected using WinSpec/32 software and an acquisition time of 30 seconds and 921 µW laser power at the sample.

Concentration Dependence Studies

Samples were prepared in 1-mL glass vials containing between 1 and 10-µL centrifuged (30 minutes, 13.4k rpm) AgNP. Two different concentration dependence series were performed to determine the optimal relative AgNP concentration for each synthesis: 1) citrate concentration dependence experiment and 2) an analyte concentration dependence experiment. The diluent for both experiments was ultrapure water. Each sample contained a final volume of 500 µL. Rhodamine B (RB) was used as a preliminary model for RB-DIA. For the RB concentration dependence experiments, 10-µL of the 10^{-4} M RB solution was added to each vial. SERS intensities for citrate at ~1400 cm^{-1} and RB at ~1650 and ~625 cm^{-1} peaks were plotted at relative concentrations to determine optimum relative concentration for each pH sensing experiment.

pH Sensing

RB-DIA dye solid (closed form) was supplied by the Harbron research lab (William & Mary, Chemistry Department). Due to the relative insolubility of RB-DIA in water, the RB-DIA solution was prepared in 2:1 water:ethanol with a final dye concentration of 1.67×10^{-3} M. Each sample was prepared in a 1-mL glass vial containing 10-µL of RB-DIA working solution, 1 to 5-µL of AgNP (based on concentration dependence experiment results) and MilliQ water up to a total volume of 500-µL. Sulfuric acid (0.01 M) and sodium hydroxide (0.01 M) were

used to adjust solution pH (Oakton pH 2700 pH meter). A Boltzmann sigmoidal fit was applied to the SERS intensity data in OriginPro 9.1 software.

Results and Discussion

Concentration Dependence Studies

The concentration dependence experiment was designed to address the variation from synthesis-to-synthesis with our citrate-reduced silver nanoparticles. Particle size, shape, and concentration can vary between syntheses and each influence the scattering intensity. The concentration dependence experiment was created to account for the concentration effects. The purpose was to determine the optimum relative nanoparticle concentration for a series of solution phase experiments. The concentration with the highest SERS intensity relative to the baseline was designated as the optimum relative concentration at neutral pH. For example, in one synthesis, the optimal AgNP concentration was 1-μL in a total volume of 500-μL or 0.20% v/v because the highest peak intensity is observed at this relative volume, as shown in Figure 3.

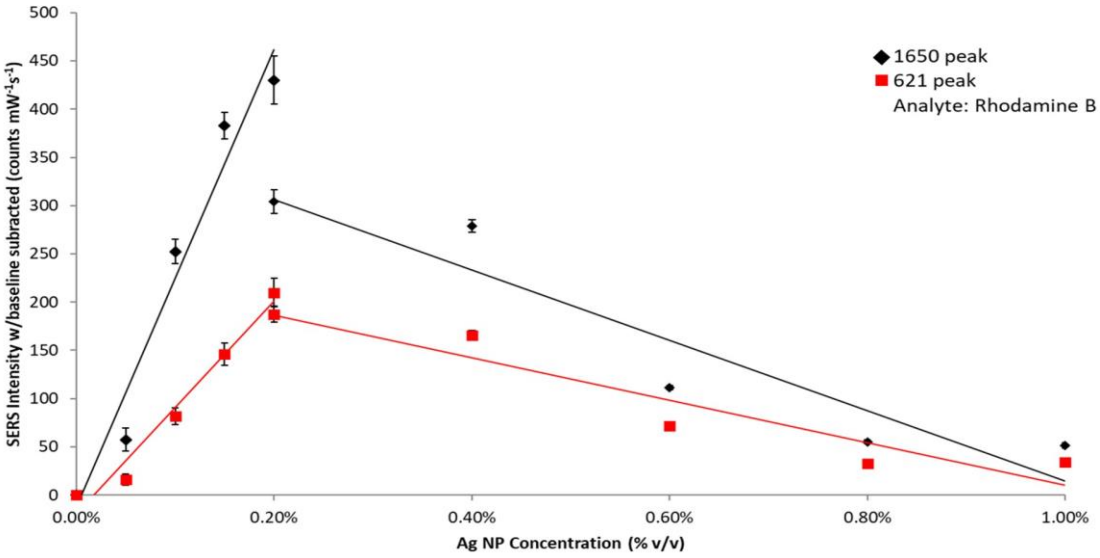

Figure 3. Concentration dependence experiment with RB showing maximum peak intensities at 0.20% v/v. Trend lines added to visualize.

The optimal relative concentrations of AgNP ranged from 0.20% to 1.0% across syntheses. This shows the variation between SERS intensity from batch-to-batch and provides a method to compensate for that variation in solution phase experiments.

pH Sensing

We conducted comparative investigations into SERS Intensity and pH effects to develop a SERS pH probe. The SERS spectrum and pH of the neutral RB-DIA/AgNP solution were collected prior to addition of acid or base. We adjusted the pH of the sample solution from neutral to basic (pH ~10). We then

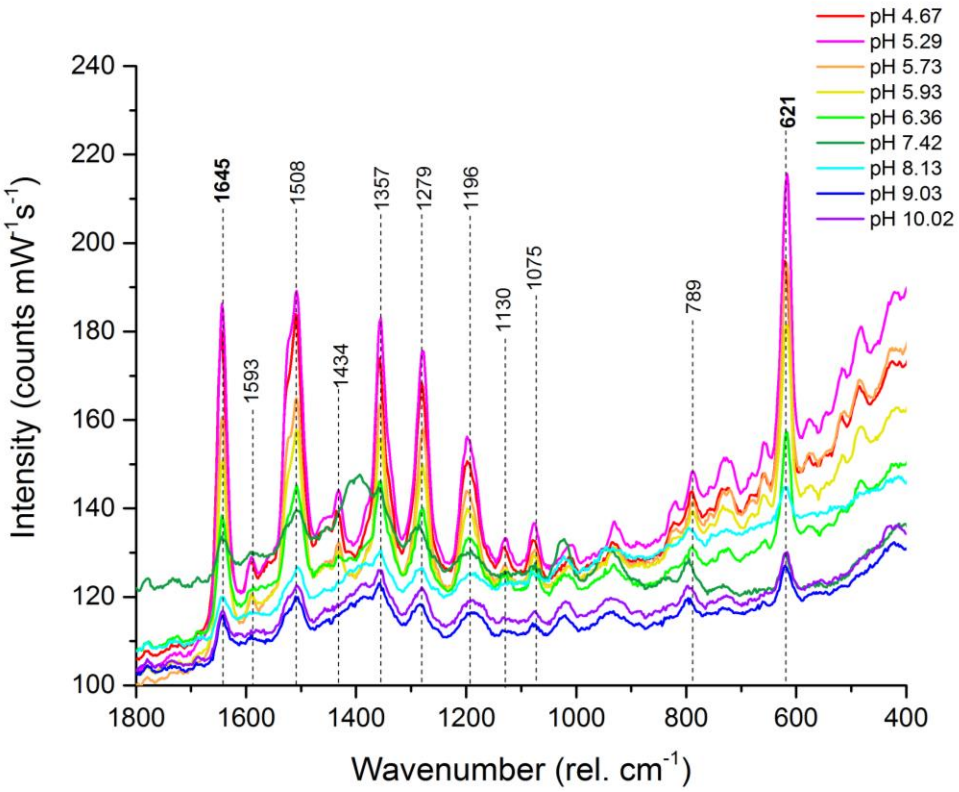

Figure 4. Overlaid spectra of the RB-DIA/AgNP pH probe response to changing pH in solution.

decreased the pH in roughly whole pH unit increments to pH ~2-3. We followed this pattern due to the observed AgNP deactivation once at acidic ranges (pH 4-3) causing the AgNP to crash out of solution.[33] For every pH increment, the SERS spectrum and pH of the RB-DIA/AgNP solution were collected. The ~1650 and ~620 cm^{-1} peak baseline-subtracted intensities for the RB-DIA/AgNP solution were plotted according to pH of the solution to determine the pH probe kinetics in solution as a metric for pH probe response (Figure 5), including the calculation of the p*K*a from Equation 1. A Boltzmann sigmoidal fit

was applied to the pH SERS plot to define the parameters in calculating the p*K*a, where *A1* is the I_{max} and *A2* is the I_{min}.

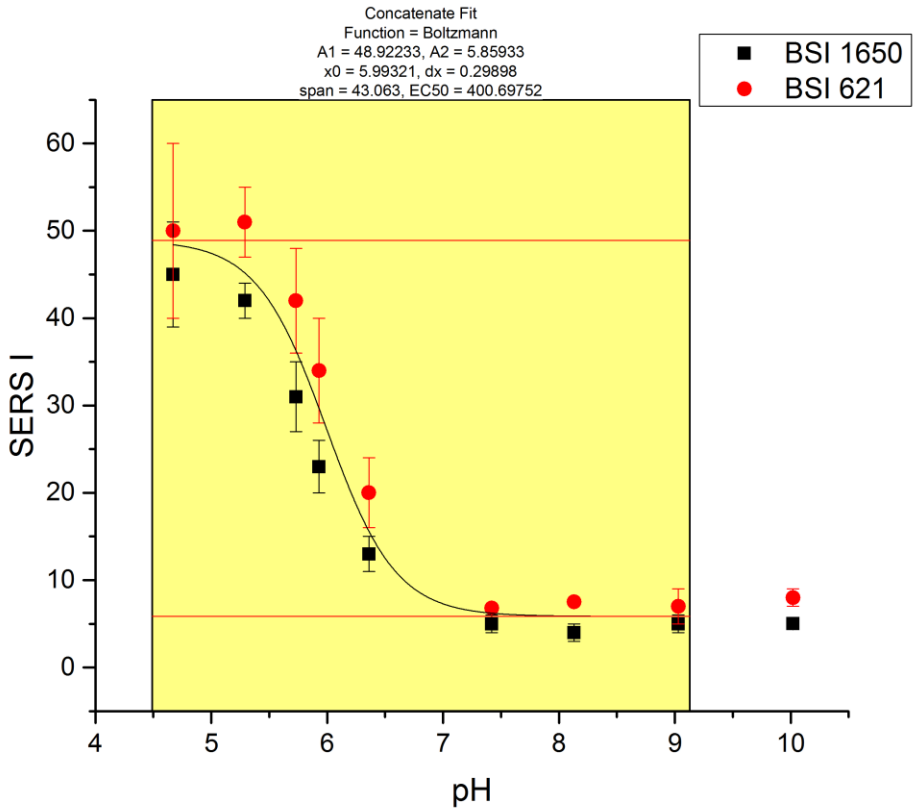

Figure 5. Boltzmann sigmoidal fitting to SERS pH data.

The calculated p*K*a was 5.8 ±0.1, which was within the standard error range of the p*K*a calculated via fluorescence from the Harbron group (p*K*a 5.7 ±0.1).[29] However, the reproducibility of results over several trials to assess the predictive power of the model was difficult. When we evaluated the SERS intensity by the Boltzmann model as a predictive model of pH (Figure 6), the error was significant.

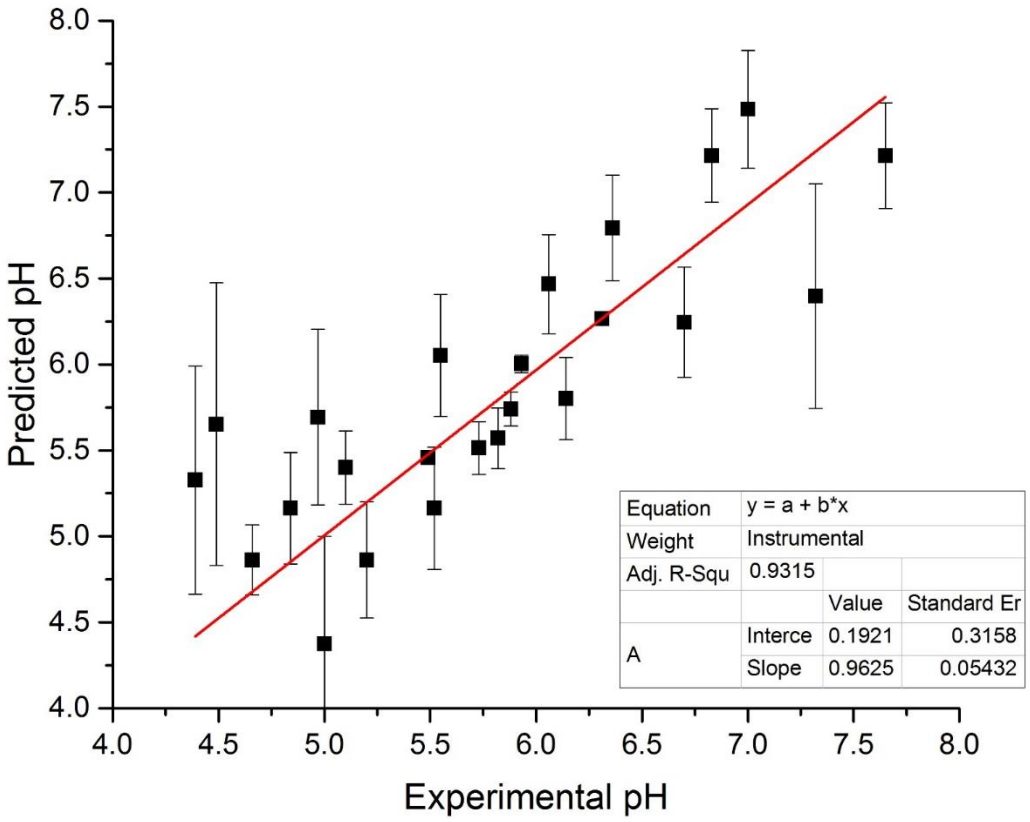

Figure 6. Evaluation of the predicted pH values by Boltzmann model calculations to the actual experimental pH values.

Another significant complication was observed with the RB control experiment yielding relatively the same p*K*a (5.7 ±0.8) as RB-DIA and similar SERS pH plots, Figure 7. The literature p*K*a value for RB is 3.1.[34] This revelation pointed towards another phenomenon confounding the results.

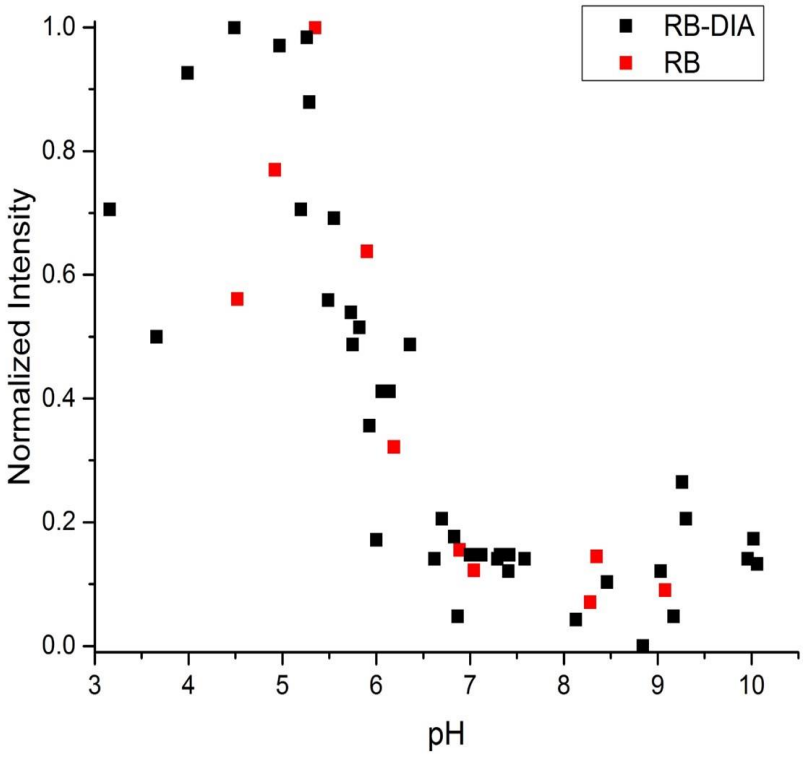

Figure 7. Overlaid SERS intensity by pH data for RB-DIA/AgNP (black) and RB/AgNP (red).

Generally, as the pH is decreased in solution, the SERS intensity increases. This is attributed to the increased population of open SERS active RB-DIA^{+}. However, the electrostatic interactions between the RB-DIA and AgNP also affect intensity with the change of pH. The Aroca group studied the affect of pH on SERS intensity of citrate-reduced AgNP combined with measured zeta(ζ)-potentials to show the change in relative surface charge as localized pH is changed.[33] The citrate capping agent makes the nanoparticle negatively charged.

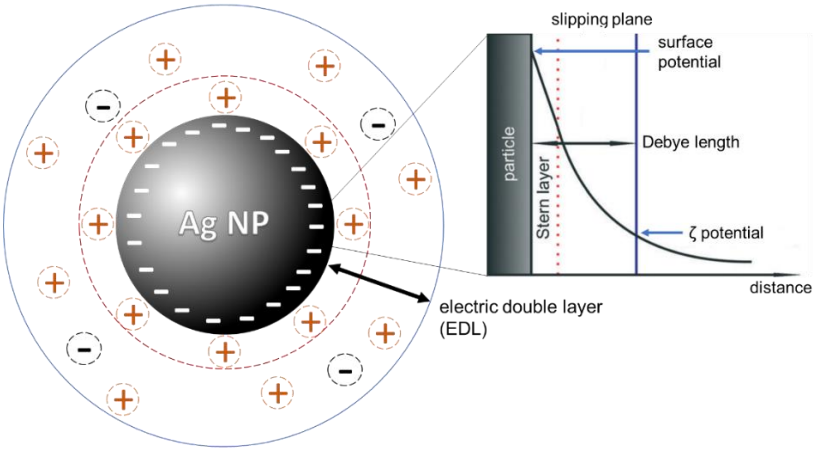

Figure 8. Diagram of nanoparticle surface charges and potentials across the electric double layer (EDL).

The ζ-potential is measured at the slipping plane (Figure 8) via dynamic light scattering (DLS), which is used to elucidate the surface charge and the relative particle stability in solution. [33] Understanding the surface charge provides insight into analyte affinity towards the AgNP. The SERS intensity increases as the RB-DIA^{+} concentration increase. However, RB is not undergoing the same structural dynamic yet still offers a similar SERS response. The RB-DIA affinity towards the nanoparticle should be investigated further to understand the underlying mechanism affecting SERS intensity. RB has an overall positive charge, which explains the similar electrostatic response to the AgNP as observed with RB-DIA. However, the spatial dependence between dye and substrate and surface charge effects on SERS intensity should be pursued by dynamic light scattering (DLS) studies to address complications.

Conclusion and Future Work

At the beginning of this work, it was hypothesized that the analyte dye RB-DIA would indicate pH sensitivity by reversible protonation/deprotonation. However, electrostatics play a critical role in the pH-dependent SERS study. Though this was not the intention at the onset, the observed SERS pH sensor response is indicative of the electrostatic interactions at the nanoparticle surface and, therefore, has the potential to be used to probe ζ-potential.

In future work, there are two different paths leading from this project. The first pathway is further study of the electrostatic interactions between AgNPs and analyte dyes to create an accurate method for characterizing the ζ-potential. Additionally, this would assist in providing another metric for particle stability in AgNP colloidal suspensions. Secondly, the electrostatic effects can be blocked to examine the protonation/deprotonation of RB-DIA. RB-DIA can be covalently attached by thiolation to the nanoparticle surface to act as a molecular tether to circumvent electrostatic complications. Preliminary results show that thiol attachment without the analyte dye does not produce a change in SERS intensity as a function of pH, Figure 9.

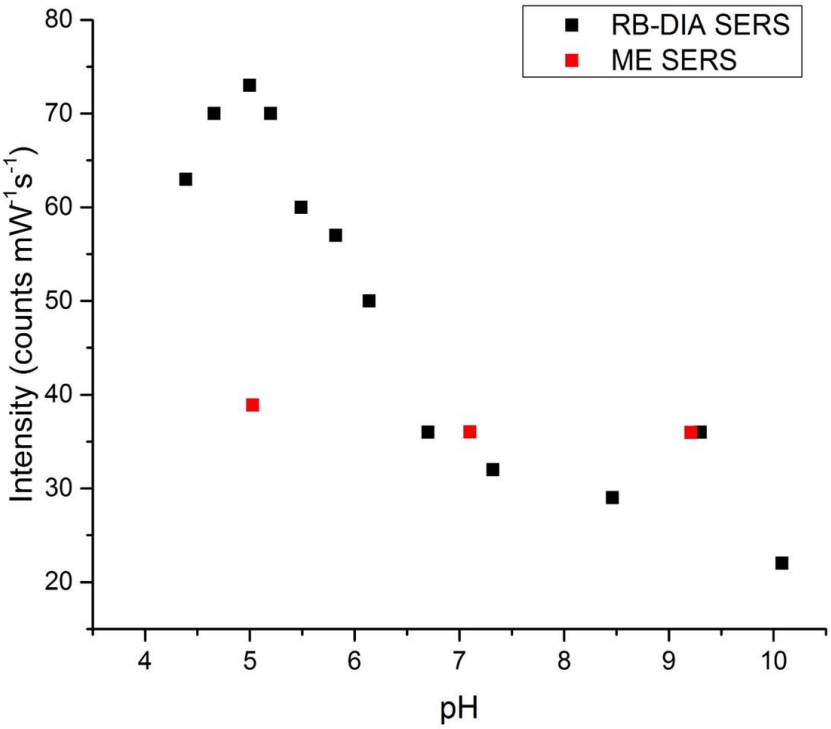

Figure 9. 2-Mercaptoethanol functionalized AgNP (red) compared to RB-DIA (black).

References

1. João Conde; João Rosa; João C. Lima; Pedro V. Baptista Nanophotonics for Molecular Diagnostics and Therapy Applications. *Int. J. Photoenergy* **2012***, 2012*, 1-11.
2. Chanda Ranjit Yonzon; Christy L Haynes; Xiaoyu Zhang; Joseph T Walsh Jr; Richard P Van Duyne A glucose biosensor based on surface-enhanced Raman scattering: Improved partition layer, temporal stability, reversibility, and resistance to serum protein interference. *Analytical Chemistry* **2004***, 76*, 78-85.
3. Rodríguez-Lorenzo, L.; Alvarez-Puebla, R. A.; Pastoriza-Santos, I.; Mazzucco, S.; Stéphan, O.; Kociak, M.; Liz-Marzán, L. M.; García de Abajo, F Javier Zeptomol detection through controlled ultrasensitive surface-enhanced Raman scattering. *Journal of the American Chemical Society* **2009***, 131*, 4616.
4. Stuart, D. A.; Yuen, J. M.; Shah, N.; Lyandres, O. In Vivo Glucose Measurement by Surface-Enhanced Raman Spectroscopy. *Analytical Chemistry* **2006***, 78*, 7211-7215.
5. Ma, K.; Yuen, J. M.; Shah, N. C.; Walsh Jr., J. T.; Glucksberg, M. R.; Van Duyne, R. P. In Vivo, Transcutaneous Glucose Sensing Using Surface-Enhanced Spatially Offset Raman Spectroscopy: Multiple Rats, Improved Hypoglycemic Accuracy, Low Incident Power, and Continuous Monitoring for Greater than 17 Days. *Anal. Chem.* **2011***, 83*, 9146.
6. Barhoumi, A.; Zhang, D.; Tam, F.; Halas, N. J. Surface-enhanced Raman spectroscopy of DNA. *Journal of the American Chemical Society* **2008***, 130*, 5523-5529.
7. Cho, H.; Lee, B.; Liu, G. L.; Agarwal, A.; Lee, L. P. Label-free and highly sensitive biomolecular detection using SERS and electrokinetic preconcentration. *Lab on a chip* **2009***, 9*, 3360.
8. Papadopoulou, E.; Bell, S. E. J. Label-Free Detection of Single-Base Mismatches in DNA by Surface-Enhanced Raman Spectroscopy. *Angewandte Chemie* **2011***, 123*, 9224-9227.
9. Chen, Y.; Chen, G.; Feng, S.; Pan, J.; Zheng, X.; Su, Y.; Chen, Y.; Huang, Z.; Lin, X.; Lan, F.; Chen, R.; Zeng, H. Label-free serum ribonucleic acid analysis for colorectal cancer detection by surface-enhanced Raman spectroscopy and multivariate analysis. *Journal of Biomedical Optics* **2012***, 17*, 067003.
10. Kwangsu Ock; Won Il Jeon; Erdene Ochir Ganbold; Mira Kim; Jinho Park; Ji Hye Seo; Keunchang Cho; Sang-Woo Joo; So Yeong Lee Real-Time Monitoring of Glutathione-Triggered Thiopurine Anticancer Drug Release in Live Cells Investigated by Surface-Enhanced Raman Scattering. *Analytical Chemistry* **2012***, 84*, 2172.
11. Kang, B.; Afifi, M. M.; Austin, L. A.; El-Sayed, M. A. Exploiting the nanoparticle plasmon effect: observing drug delivery dynamics in single

cells via Raman/fluorescence imaging spectroscopy. *ACS nano* **2013***, 7*, 7420.
12. Kircher, M. F.; De La Zerda, A.; Jokerst, J. V.; Zavaleta, C. L.; Kempen, P. J.; Mittra, E.; Pitter, K.; Huangm, R.; Campos, C.; Habte, F.; Sinclair, R.; Brennan, C. W.; Mellinghoff, I. K.; Holland, E. C.; Gambhir, S. S. A brain tumor molecular imaging strategy using a new triple-modality MRI-photoacoustic-Raman nanoparticle. *Nat. Med.* **2012***, 18*, 829-834.
13. Zaleski, S.; Cardinal, M. F.; Chulhai, D. V.; Wilson, A. J.; Willets, K. A.; Jensen, L.; Van Duyne, R.,P. Toward Monitoring Electrochemical Reactions with Dual-Wavelength SERS: Characterization of Rhodamine 6G (R6G) Neutral Radical Species and Covalent Tethering of R6G to Silver Nanoparticles. *J. Phys. Chem.* **2016***, 120*, 24982-24991.
14. Kneipp, J.; Kneipp, H.; Wittig, B.; Kneipp, K. Following the Dynamics of pH in Endosomes of Live Cells with SERS Nanosensors. *J. Phys. Chem.* **2010***, 114*, 7421-7426.
15. Kneipp, J.; Kneipp, H.; Wittig, B.; Kneipp, K. One- and two-photon excited optical ph probing for cells using surface-enhanced Raman and hyper-Raman nanosensors. *Nano Lett.* **2007***, 7*, 2819-2823.
16. Bishnoi, S. W.; Rozell, C. J.; Levin, C. S.; Gheith, M. K.; Johnson, B. R.; Johnson, D. H.; Halas, N. J. All-optical nanoscale pH meter. *Nano Lett.* **2006***, 6*, 1687-1692.
17. Graham, D.; Faulds, K.; Smith, W. E. Biosensing using silver nanoparticles and surface enhanced resonance Raman scattering. *Chem. Commun.* **2006**, 4363-4371.
18. Taylor, J.; Huefner, A.; Li, L.; Wingfield, J.; Mahajan, S. Nanoparticles and intracellular applications of surface-enhanced Raman spectroscopy. *Analyst* **2016***, 141*, 5037-5055.
19. Piotrowski, P.; Wrzosek, B.; Królikowska, A.; Bukowska, J. A SERS-based pH sensor utilizing 3-amino-5-mercapto-1,2,4-triazole functionalized Ag nanoparticles. *Analyst* **2014***, 139*, 1101-1111.
20. Ngo, H. T.; Wang, H.; Fales, A. M.; Vo-Dinh, T. Plasmonic SERS biosensing nanochips for DNA detection. *Anal. Bioanal. Chem.* **2016***, 408*, 1773-1781.
21. Howes, P. D.; Chandrawati, R.; Stevens, M. M. Bionanotechnology. Colloidal nanoparticles as advanced biological sensors. *Science (New York, N.Y.)* **2014***, 346*, 1247390.
22. Howes, P.; Rana, S.; Stevens, M. Plasmonic nanomaterials for biodiagnostics. *Chem. Soc. Rev.* **2014***, 43*, 3835-3853.
23. Wei, H.; Hossein Abtahi, S. M.; Vikesland, P. J. Plasmonic colorimetric and SERS sensors for environmental analysis. *Environ. Sci.: Nano* **2015***, 2*, 12-135.
24. Sikkandhar, M. G.; Nedumaran, A. M.; Ravichandar, R.; Singh, S.; Santhakumar, I.; Goh, Z. C.; Mishra, S.; Archunan, G.; Gulyas, B.;

Padmanabhan, P. Theranostic Probes for Targeting Tumor Microenvironment: An Overview. *Int. J. Mol. Sci.* **2017***, 18*, 1036.
25. Chen, J.; Chen, C.; Chang, C. A fluorescent pH probe for acidic organelles in living cells. *Org. Biomol. Chem.* **2017***, 15*, 7936-7943.
26. Nakata, E.; Yukimachi, Y.; Kariyazono, H.; Im, S.; Abe, C.; Uto, Y.; Maezawa, H.; Hashimoto, T.; Okamoto, Y.; Hori, H. Design of a bioreductively-activated fluorescent pH probe for tumor hypoxia imaging. *Bioorganic & Medicinal Chemistry* **2009***, 17*, 6952-6958.
27. Song, P.; Chen, X.; Xiang, Y.; Huang, L.; Zhou, Z.; Wei, R.; Tong, A. A ratiometric fluorescent pH probe based on aggregation-induced emission enhancement and its application in live-cell imaging. *Journal of Materials Chemistry* **2011***, 21*, 13470.
28. Schulte, A.; Lorenzen, I.; Böttcher, M.; Plieth, C. A novel fluorescent pH probe for expression in plants. *Plant methods* **2006***, 2*, 7.
29. Czaplyski, W. L.; Purnell, G. E.; Roberts, C. A.; Allred, R. M.; Harbron, E. J. Substituent effects on the turn-on kinetics of rhodamine-based fluorescent pH probes. *Org. Biomol. Chem.* **2014***, 12*, 526-533.
30. Stiles, P. L.; Dieringer, J. A.; Shah, N. C.; Van Duyne, R. P. Surface-Enhanced Raman Spectroscopy. *Annu. Rev. Anal. Chem.* **2008***, 1*, 601-626.
31. Liu, L.; Guo, P.; Chai, L.; Shi, Q.; Xu, B.; Yuan, J.; Wang, X.; Shi, X.; Zhang, W. Fluorescent and colorimetric detection of pH by a rhodamine-based probe. *Sensors and Actuators B: Chemical* **2014***, 194*, 498-502.
32. Lee, P. C.; Meisel, D. Adsorption and surface-enhanced Raman of dyes on silver and gold sols. *J. Phys. Chem.* **1982**, 3391-3395.
33. Alvarez-Puebla, R. A.; Arceo, E.; Goulet, P. J. G.; Garrido, J. J.; Aroca, R. F. Role of nanoparticle surface charge in surface-enhanced Raman scattering. *J. Phys. Chem. B* **2005***, 109*, 3787-3792.
34. Lopez Arbeloa, F.; Lopez Arbeloa, T.; Tapia Estevez, M. J.; Lopez Arbeloa, I. Photophysics of rhodamines: molecular structure and solvent effects. *J. Phys. Chem.* **1991***, 95*, 2203-2208.